GENERATION, COMPRESSION, QUASISTATIC DEFORMATION OF MODEL GRANULAR MATERIALS

grain-level simulations, micromechanical approaches

Role of microscopic model ingredients, definition of relevant variables and control parameters

Jean-Noël ROUX

Laboratoire Navier, Université Paris-Est, France

SCOPE: assembling processes for granular packings, isotropic (or oedometric compression), elastic properties, small to moderate strains in response to deviatoric loads.

Model systems: assemblies of spherical beads (or disks in 2D)

ISOTROPIC COMPRESSION

Solid fraction and coordination number in isotropic pressure cycle

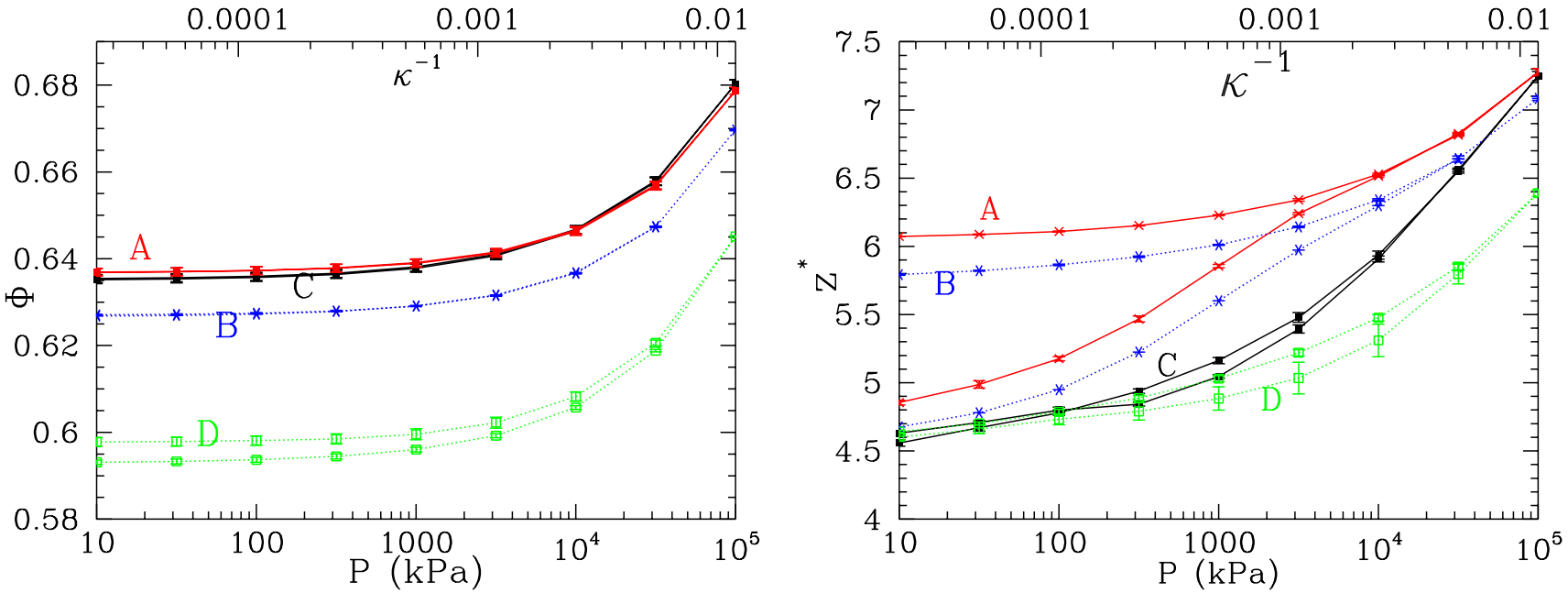

Initially isotropic states A, B, C, D. Very nearly reversible for Φ, not reversible for z^*, which decreases if initially high.

Similar behaviour in systems assembled by pluviation.

Normal force distribution under growing pressure

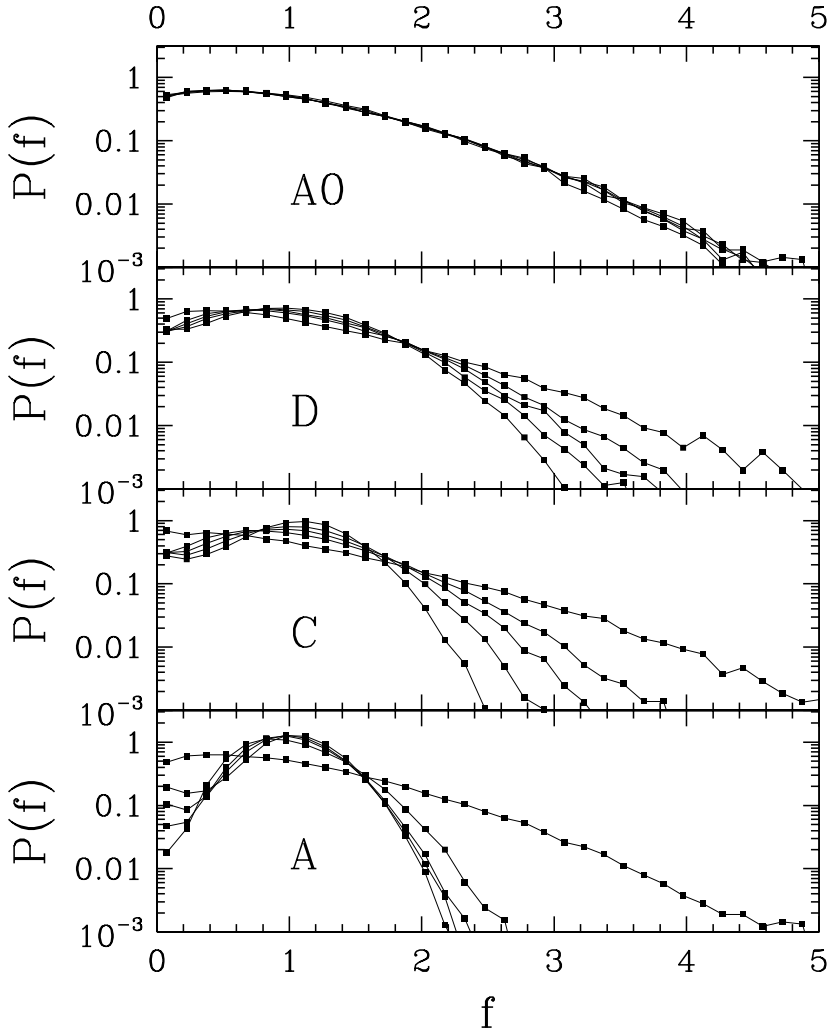

$f = F_N/\langle F_N \rangle$,

$P = 10, 100, 10^3, 10^4, 10^5$ kPa

Distribution narrows as force indeterminacy increases.

A0 = frictionless system. A=A0 in initial state

A is frictional, assembled without friction.

Confinement conserves inherent fabric anisotropy...

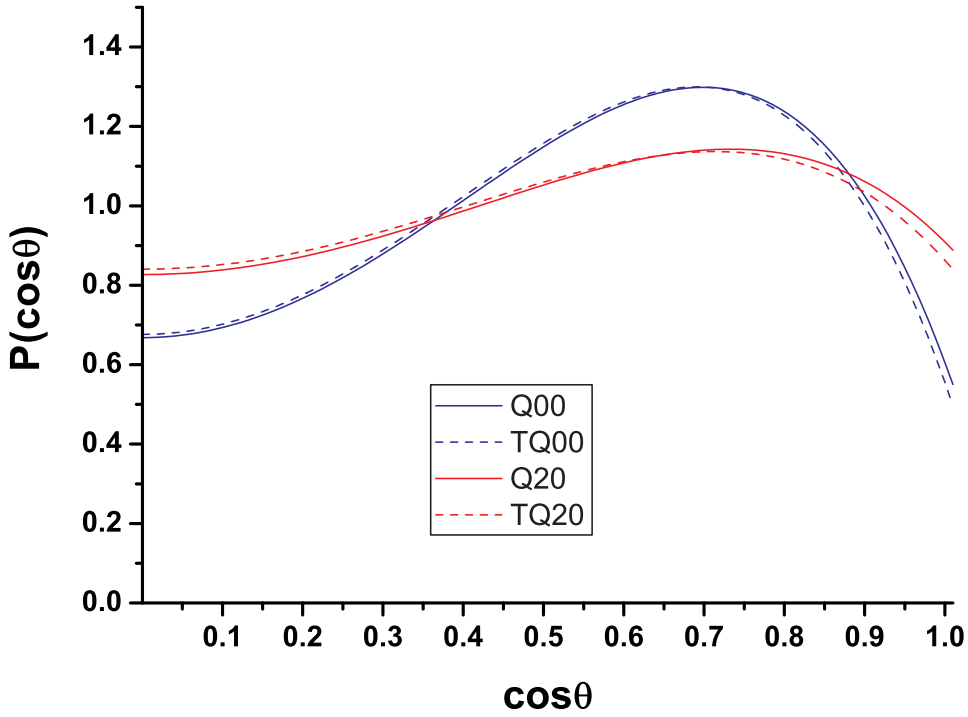

... even though initial stresses were anisotropic

2 systems made by pluviation, same Q^*, different H_p^* (0 and 20)

Continuous line = inherent anisotropy after pluviation

Dotted line = anisotropy after application of isotropic pressure

Plastic compaction of cohesive system

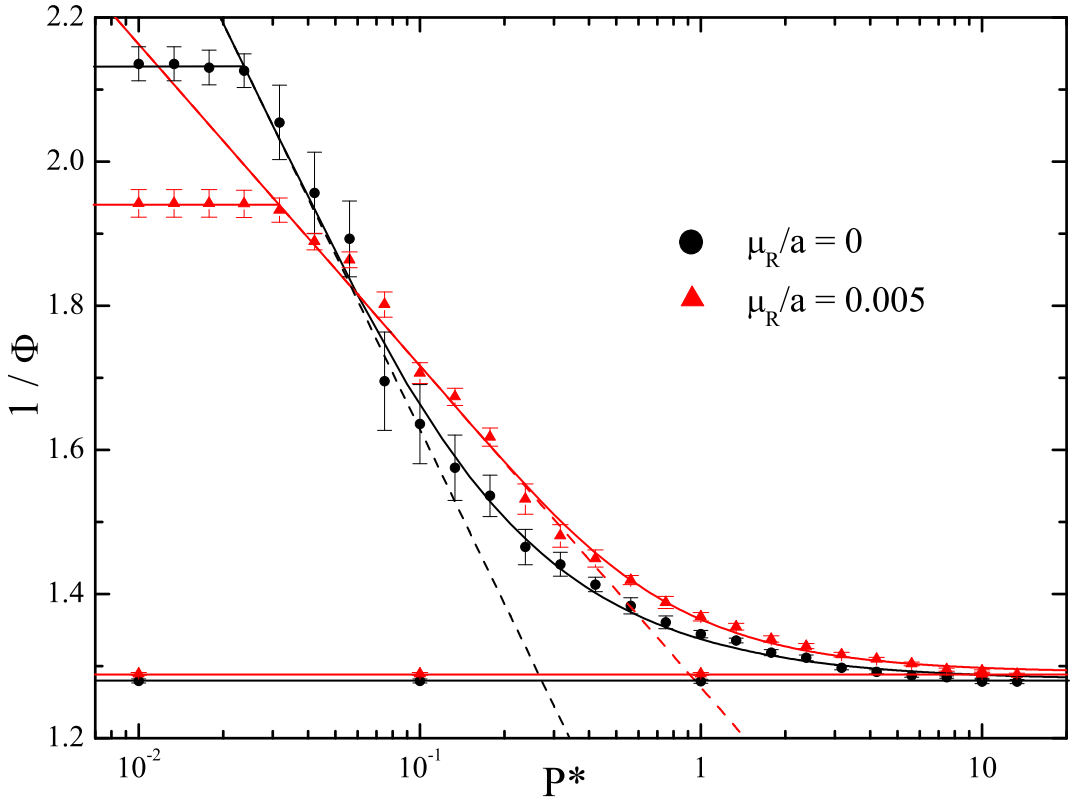

Under growing P^* open, tenuous contact networks irreversibly collapse.

Definition of $P^* \rightarrow$ correct pressure range where plastic collapse occurs

Note influence of small RR. Void index varies linearly with $\ln P^*$ as in traditional presentation of “consolidation curves”.

Cohesive system under high P^*: maximum consolidation

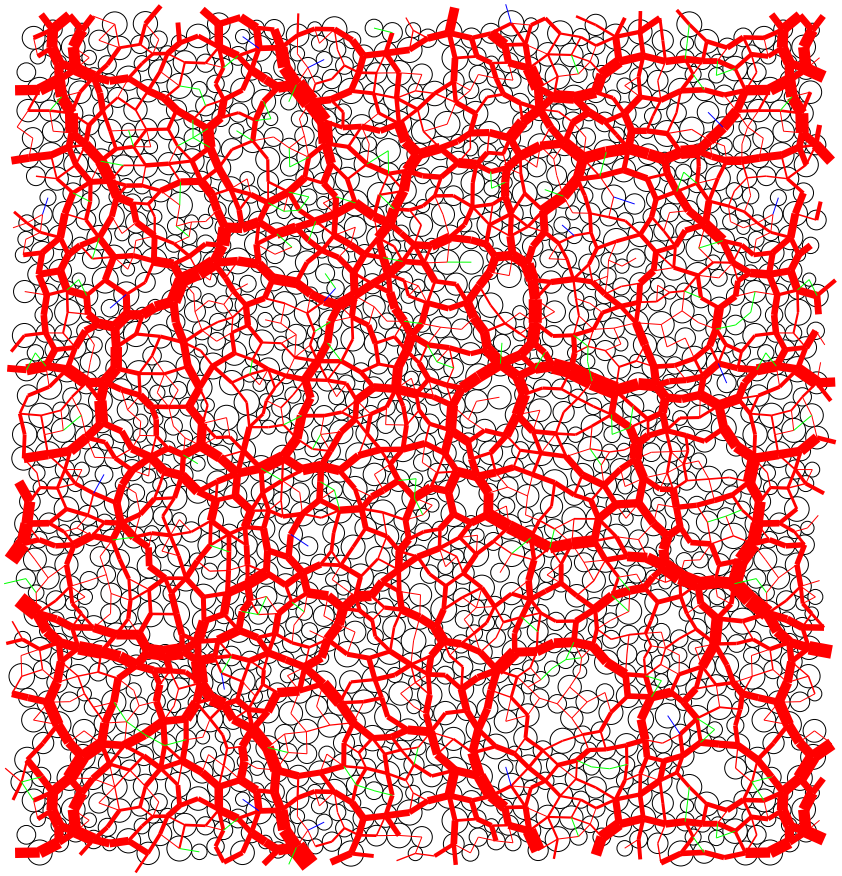

Repulsive forces only, similar force chains and density as in cohesionless systems.

Cohesive system under low P^* after pressure cycle

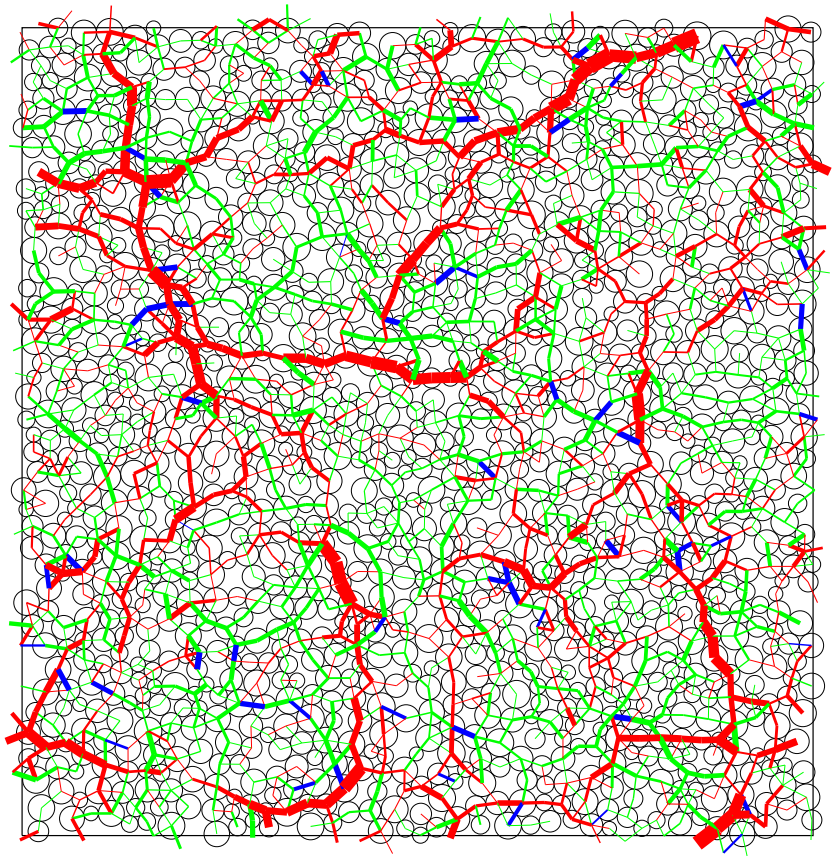

Compensation of tensile and compressive forces again

Strong compressive chains, more numerous tensile ones forming “tension only” domains

Blue lines = distant attractions

How can one obtain truly loose packings of beads ?

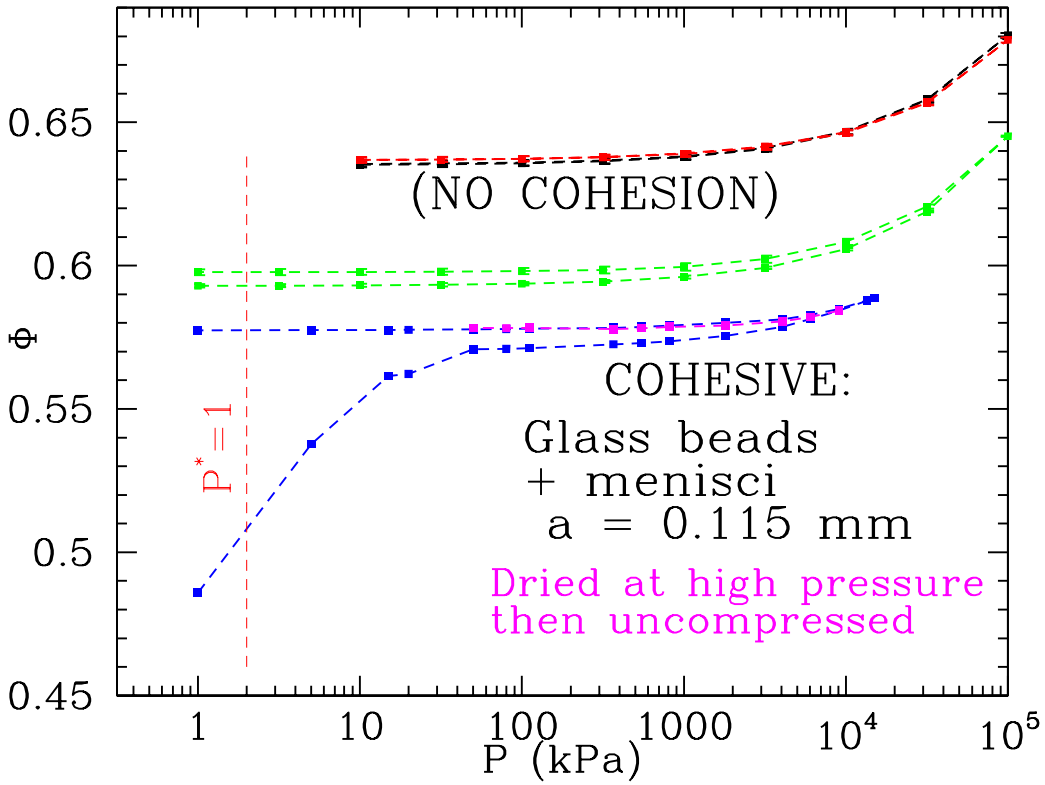

Suppress capillary cohesion at high P^*, then uncompress $\Rightarrow$ lower density

In the lab, moist tamping procedure to make loose configurations

“Loose random packing”: no definition independent on procedure and contact law !

Some conclusions on preparation process and confinement of solid granular samples

- Density alone not enough to classify packings: coordination number may change a lot for dense samples Extreme cases obtained with (idealised) lubrication and with (idealised) vibration
- Compacting = avoiding the effects of friction
- Moderate anisotropy in simulations of pluviation (coordination similar to partially lubricated case)
- Cohesive systems exhibit a much wider variety of structures, form loose structures with different degrees of branching... Assembling stage bound to depend on effects of surrounding fluid in practice
- Effect of compression in cohesionless systems: significantly affects system geometry as κ decreases to $\sim 10^3$
- Pressure cycle: little irreversibility for density, important effect on coordination number
- With cohesion: plastic collapse, ruled by P^*, with $\Delta(1/\Phi) \propto -\Delta \ln P^*$
- Quantitative comparisons to experiments? $\Rightarrow$ elastic properties

PROPERTIES
OF CONTACT NETWORKS

Definitions: system, load

N grains in dimension $d \Rightarrow Nd(d+1)/2$ degrees of freedom, displacements $\mathbf{u}_i$ and (small) rotations $\vec{\theta}_i$, $1 \leq i \leq N$. In general, boundary conditions (walls, periodic boundaries...), global degrees of freedom contribute $n_g \ll N$ DOF $\rightarrow N_f = Nd(d+1)/2 + n_g$ degrees of freedom, assembled in a grand displacement vector $\mathbf{U}$, with N_f coordinates.

The load vector $\mathbf{F}^{\text{ext}}$ gathers all components of external forces $\mathbf{F}_i^{\text{ext}}$ and moments $\mathbf{\Gamma}_i^{\text{ext}}$ exerted on the grains i and conjugate forces to the n_g boundary or collectife DOF's.

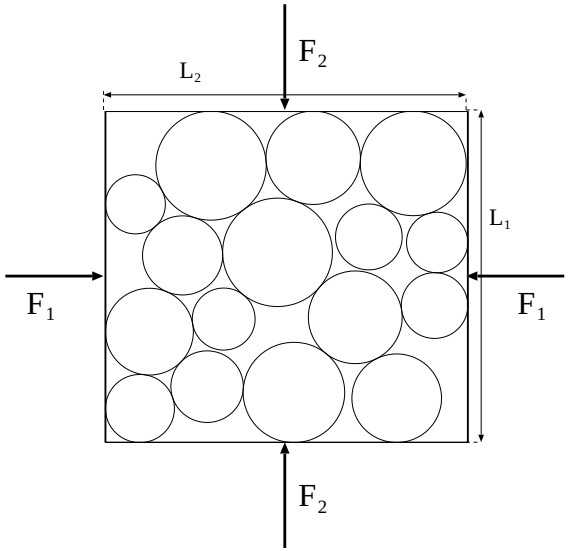

2D biaxial test, with 2 mobile walls, 2 fixed ones, or opposite walls requested to have opposite velocities

$\Rightarrow n_g = 2$

Relative displacements and rigidity matrix $\underline{\underline{G}}$

Define in each one of N_c contacts (or interactions across small interstices) a "first" grain, say i and a second one, say j. The relative displacement is

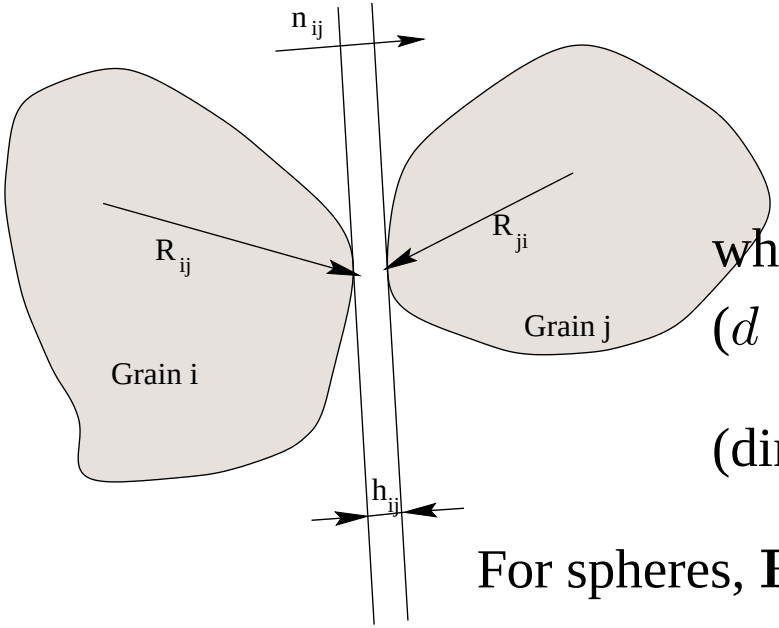

$$\vec{\mathcal{U}}_{ij} = \mathbf{u}_i - \mathbf{u}_j + \vec{\theta}_i \wedge \mathbf{R}_{ij} - \vec{\theta}_j \wedge \mathbf{R}_{ji},$$

which defines the rigidity matrix $\underline{\underline{\mathbf{G}}}$
($d \times N_c$ rows in dimension d, N_f columns)

$$(\text{dim . } N_f)\ \mathbf{U} \mapsto \underline{\underline{G}} \cdot \mathbf{U} = \vec{\mathcal{U}} \ (\text{ dim. } 3N_c \text{ in 3D})$$

For spheres, $\mathbf{R}_{ij} = R_i \mathbf{n}_{ij}$, $\mathbf{R}_{ji} = -R_j \mathbf{n}_{ij}$ and

$$\vec{\mathcal{U}}_{ij} = \mathbf{u}_i - \mathbf{u}_j + (R_i \vec{\theta}_i + R_j \vec{\theta}_j) \wedge \mathbf{n}_{ij}$$

We introduced branch vectors (arbitrary grain centre in general) and normal unit vectors at contacts.

Properties of rigidity matrix $\underline{\underline{G}}$

- "Mechanism" motions: $\mathbf{U}$ such that $\underline{\underline{G}} \cdot \mathbf{U} = 0. \rightarrow k$-dimensional space, k=degree of displacement indeterminacy, kernel of $\underline{\underline{G}}$. Includes global rigid-body motions.
- Compatibility of relative displacements: condition that $\vec{\mathcal{U}}$ corresponds to some displacement vector $\mathbf{U}$ by $\underline{\underline{G}}$
  Range of $\underline{\underline{G}}$, dimension $N_f - k$.

(We use an assumption of small displacements (**ASD**)
($\mathbf{n}_{ij}$, $\mathbf{R}_{ij}$ constant, displacements dealt with as infinitesimal, or like velocities)

Contact forces and equilibrium equations

In each contact define the contact force $\mathbf{f}_{ij}$ as the one transmitted by the "first" grain to the "second" one

Equilibrium condition = linear relation between contact forces and external load

$$\mathbf{F}_i^{\text{ext}} = \sum_{j \neq i} \mathbf{f}_{ij}$$

$$\mathbf{\Gamma}_i^{\text{ext}} = \sum_{j \neq i} \mathbf{f}_{ij} \wedge \mathbf{R}_{ij}$$

If $\mathbf{f}$ is the vector of contact forces, $\mathbf{F}^{\text{ext}}$ the applied load, then

$$\mathbf{F}^{\text{ext}} = \underline{\underline{H}} \cdot \mathbf{f} \quad (dN_c\text{-dimensional vectors})$$

- Self-balanced contact forces: $\mathbf{f}$ such that $\underline{\underline{H}} \cdot \mathbf{f} = 0$. $\rightarrow$ kernel of $\underline{\underline{H}}$, space of dimension h, degree of force indeterminacy.
- Supportable loading vector = $\mathbf{F}^{\text{ext}}$ corresponding to some contact force vector $\mathbf{f}$ by $\underline{\underline{H}} \rightarrow$ range of $\underline{\underline{H}}$, dimension $dN_c - h$

Remarks on rigidity matrices

- For $\mathbf{f}$ and $\vec{\mathcal{U}}$, distinguish **normal and tangential parts** (convenient coordinates in dN_c spaces of contact forces in relative displacements)
- With frictionless contacts **ignore tangential components**
- The rigidity matrix (non-square in general, purely geometric) should not be confused with the stiffness matrix (square, involves material behaviour)
- Name *rigidity matrix* originates in *rigidity theory* (for frameworks of articulated bars, cable networks, tensegrities). Not used by ererybody... Some call $\pm\underline{\underline{H}}$ the rigidity matrix...

$\underline{\underline{H}}$ is related to $\underline{\underline{G}}$:

Theorem of virtual work and consequences

$$\boxed{\underline{\underline{H}} = \underline{\underline{G}}^T}$$

If $\mathbf{f}$, a set of contact forces, balances load $\mathbf{F}^{\text{ext}}$

If $\mathbf{U}$, displacement vector, corresponds to relative displacements $\vec{\mathcal{U}}$, then (ASD)

$$\mathbf{f} \cdot \vec{\mathcal{U}} = \mathbf{F}^{\text{ext}} \cdot \mathbf{U}$$

- Compatibility of relative displacements = orthogonality to self-balanced forces

$$\text{range}\left(\underline{\underline{G}}\right) = \left(\text{Ker}\left(\underline{\underline{H}}\right)\right)^{\perp} \quad \text{in } \mathbb{R}^{dN_c}$$

- Supportable loads = those orthogonal to mechanisms

$$\text{range}\left(\underline{\underline{H}}\right) = \left(\text{Ker}\left(\underline{\underline{G}}\right)\right)^{\perp} \quad \text{in } \mathbb{R}^{N_f}$$

- Force and displacement degrees of indeterminacy related by

$\boxed{N_f + h = dN_c + k}$ in general, or $\boxed{N_f + h = N_c + k}$ without friction

In a large system, $N_c = zN/2$ ($N =$ nb of grains).

Frictionless disks or spheres $\Rightarrow k \geq N$ (2D) or $k \geq 3N$ (3D)

ELASTIC PROPERTIES

AND SMALL STRAIN BEHAVIOUR

1. Some experimental observations
2. Simulations: incremental response of contact networks
3. Predictions of elastic moduli of model materials
4. Simulation results, comparisons simulation/theory/experiment

Elastic behaviour in granular materials, sands, geomaterials

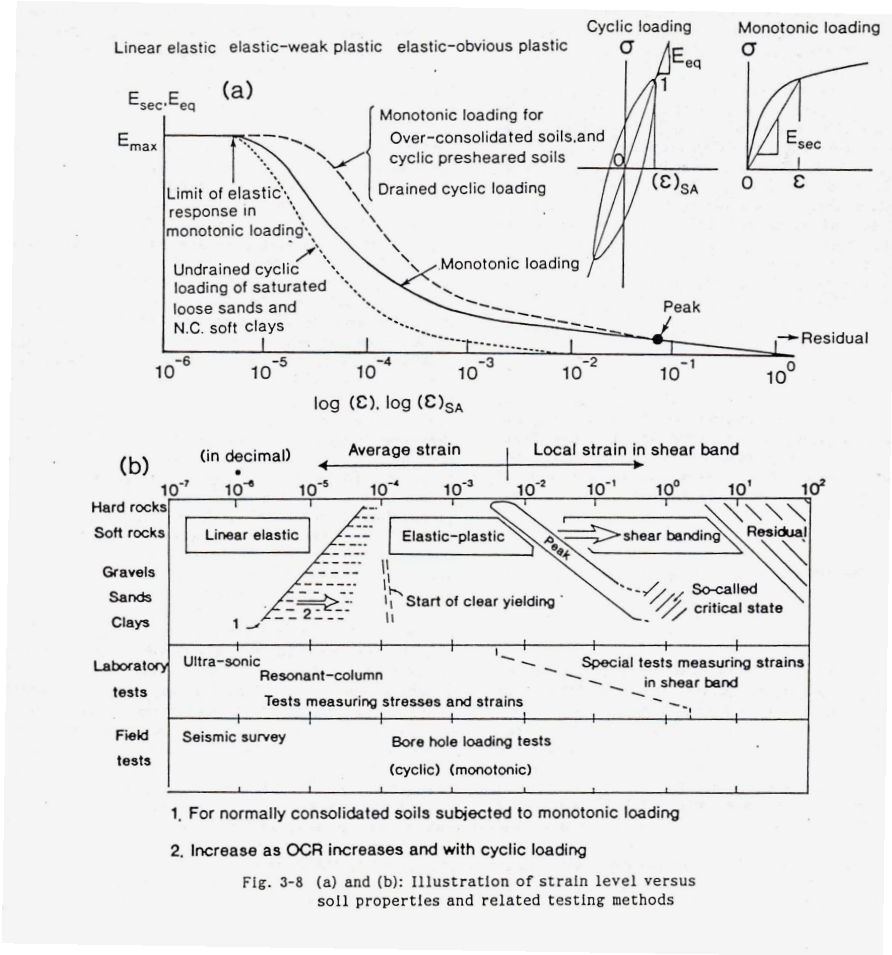

Fig. 3-8 (a) and (b): Illustration of strain level versus soil properties and related testing methods

Hoque & Tatsuoka

- *Linear* elasticity ("tangent elasticity") for small increments of strains and stresses about a prestressed state
- different methods agree when simultaneously available
- lots of data on geomaterials... less on model materials!

Static versus dynamic moduli

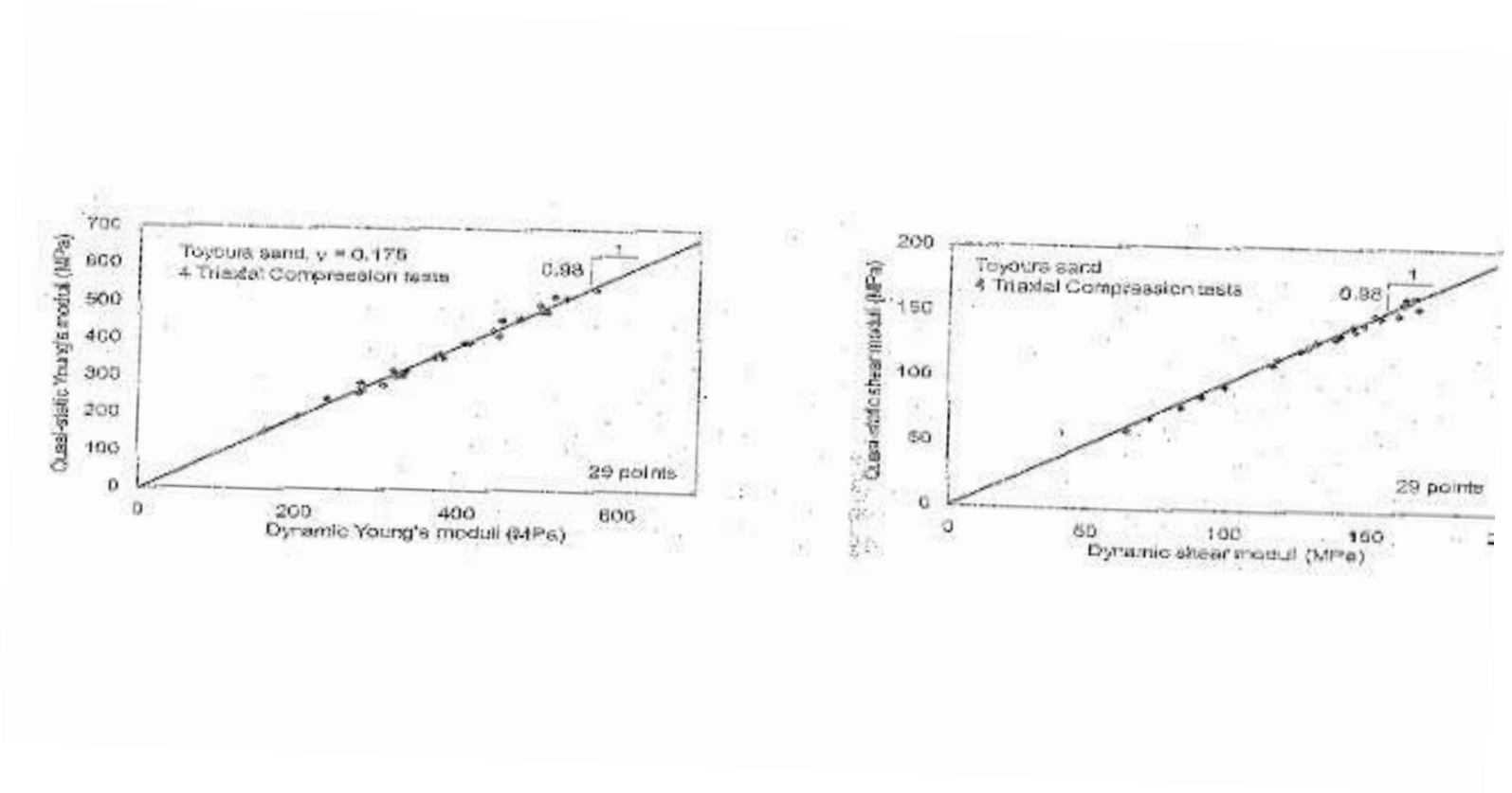

- Accurate agreement between both measurement results!
- Wave velocities for isotropic medium:

$$\text{Longitudinal: } V_P = \sqrt{\frac{C_{11}}{\rho}} = \sqrt{\frac{B + 4G/3}{\rho}} \qquad \text{Transverse: } V_S = \sqrt{\frac{G}{\rho}}$$

Measurement of elastic moduli in stress-strain test

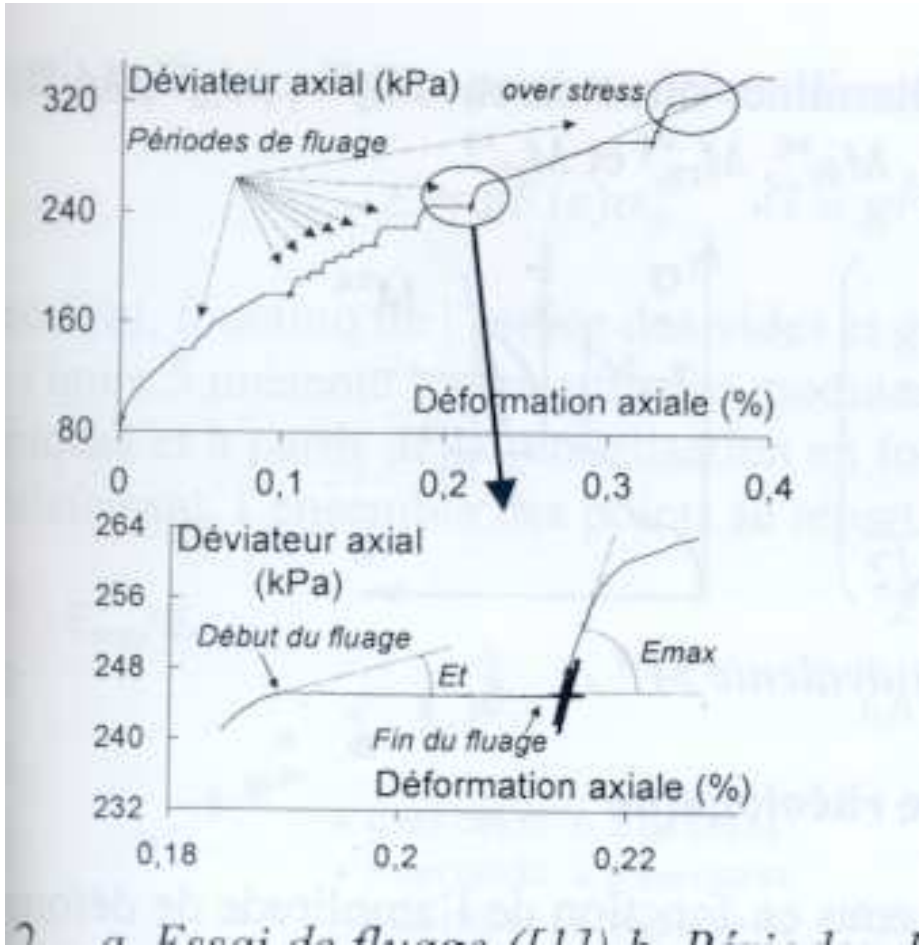

- Creep periods (constant stress) along monotonic curve in triaxial compression
- incremental response $\sim$ elastic after some creep interval of strain
- Moduli measured with cyclic load of small amplitude
- compression test resumed $\Rightarrow$ back to previous stress-strain curve

Elasticity. Isotropic case.

$$\Delta\underline{\tilde{\sigma}} = \begin{bmatrix} \Delta\sigma_{11} \\ \Delta\sigma_{22} \\ \Delta\sigma_{33} \\ \Delta\sigma_{23} \\ \Delta\sigma_{31} \\ \Delta\sigma_{12} \end{bmatrix} = \begin{bmatrix} C_{11} & C_{12} & C_{12} & 0 & 0 & 0 \\ C_{12} & C_{11} & C_{12} & 0 & 0 & 0 \\ C_{12} & C_{12} & C_{11} & 0 & 0 & 0 \\ 0 & 0 & 0 & 2C_{44} & 0 & \\ 0 & 0 & 0 & 0 & 2C_{44} & 0 \\ 0 & 0 & 0 & 0 & 0 & 2C_{44} \end{bmatrix} \cdot \begin{bmatrix} \epsilon_{11} \\ \epsilon_{22} \\ \epsilon_{33} \\ \epsilon_{23} \\ \epsilon_{31} \\ \epsilon_{12} \end{bmatrix} = \underline{\underline{\tilde{\mathbf{C}}}} \cdot \underline{\tilde{\epsilon}},$$

with:

$$C_{11} = B + \frac{4}{3}G = \lambda + 2\mu$$

$$C_{12} = \lambda$$

$$C_{44} = \mu = \frac{C_{11} - C_{12}}{2}$$

Convention: $\underline{\underline{\epsilon}} = -\frac{1}{2}\left(\underline{\underline{\nabla \mathbf{u}}} + {}^{\mathbf{T}}\underline{\underline{\nabla \mathbf{u}}}\right)$

Transversely isotropic material

Axis of coordinate x_1 particular

$$\Delta\underline{\tilde{\sigma}} = \begin{bmatrix} \Delta\sigma_{11} \\ \Delta\sigma_{22} \\ \Delta\sigma_{33} \\ \Delta\sigma_{23} \\ \Delta\sigma_{31} \\ \Delta\sigma_{12} \end{bmatrix} = \begin{bmatrix} C_{11} & C_{12} & C_{12} & 0 & 0 & 0 \\ C_{12} & C_{22} & C_{23} & 0 & 0 & 0 \\ C_{12} & C_{23} & C_{22} & 0 & 0 & 0 \\ 0 & 0 & 0 & 2C_{44} & 0 & 0 \\ 0 & 0 & 0 & 0 & 2C_{55} & 0 \\ 0 & 0 & 0 & 0 & 0 & 2C_{55} \end{bmatrix} \cdot \begin{bmatrix} \epsilon_{11} \\ \epsilon_{22} \\ \epsilon_{33} \\ \epsilon_{23} \\ \epsilon_{31} \\ \epsilon_{12} \end{bmatrix} = \underline{\underline{\tilde{\mathbf{C}}}} \cdot \underline{\tilde{\epsilon}},$$

with :

$$C_{44} = \frac{C_{22} - C_{23}}{2}$$

5 independent constants instead of 2.

Longitudinal waves in direction i, $1 \leq i \leq 3$ propagate with velocity $\sqrt{C_{ii}/\rho}$

Incremental response of contact network: local stiffness matrix

Contact laws relate contact forces $\mathbf{f}_{ij}$ to relative displacements $\vec{\mathcal{U}}_{ij}$.
Linearize for small variations $\Rightarrow$ define contact stiffness matrix $\underline{\underline{\mathcal{K}}}_{ij}$.

Using basis $\mathbf{n}_{ij},\ \mathbf{t}_{ij} = \frac{\mathbf{F}_{ij}^T}{||\mathbf{F}_{ij}^T||},\ \mathbf{w}_{ij} = \mathbf{n}_{ij} \times \mathbf{t}_{ij}$, for linear contact elasticity, one has:

$$\Delta \mathbf{f}_{ij} = \underline{\underline{\mathcal{K}}}_{ij} \cdot \Delta \vec{\mathcal{U}}_{ij},$$

If $||\mathbf{F}_{ij}^T|| < \mu \mathbf{F}_{ij}^N$, one has (*elastic form of local stiffness matrix*)

$$\underline{\underline{\mathcal{K}}}_{ij} = \underline{\underline{\mathcal{K}}}_{ij}^E = \begin{bmatrix} K_N^{ij} & 0 & 0 \\ 0 & K_T^{ij} & 0 \\ 0 & 0 & K_T^{ij} \end{bmatrix},$$

Incremental response of contact network: local stiffness matrix

If $||\mathbf{F}_{ij}^T|| = \mu \mathbf{F}_{ij}^N$, then (*elastoplastic form of local stiffness matrix*)

$$\underline{\underline{\mathcal{K}}}_{ij} = \begin{cases} \begin{bmatrix} K_N^{ij} & 0 & 0 \\ \mu K_N^{ij} & 0 & 0 \\ 0 & 0 & K_T^{ij} \end{bmatrix} & \text{if } K_T^{ij} \Delta\vec{\mathcal{U}}_{ij} \cdot \mathbf{t}_{ij} - \mu K_N^{ij} \mathbf{n}_{ij} \cdot \Delta\vec{\mathcal{U}}_{ij} > 0 \\ \underline{\underline{\mathcal{K}}}_{ij}^E & \text{otherwise} \end{cases}$$

Thus contact stiffness matrix depends on direction of $\Delta\vec{\mathcal{U}}_{ij}$ in general.

Local stiffness matrix, Hertzian case

With Hertz-Mindlin contacts,

- stiffnesses K_N, K_T depend on elastic normal force F_N.
- the contact law is always path-dependent

$\underline{\underline{\mathcal{K}}}^E_{ij}$ should be corrected

- for receding pairs (rescaling prescription for K_T),
- and, possibly, to Mindlin form involving factor $\left(1 - \frac{||\mathbf{F}_T||}{\mu F_N}\right)^{1/3}$, because of gradual friction mobilization.

Such corrections depend on direction of $\Delta\vec{\mathcal{U}}_{ij}$

Contact network elasticity is at best an approximation

(*even if no contact force reaches the edge of the Coulomb cone*)

Computations of elastic moduli ignore such corrections (energetically inconsistent with small cyclic loads).
Small error on "moduli" (below $\sim 3\%$, I. Agnolin & J.-N. Roux 2007)

Local stiffness matrices and structural stiffness matrix

One may write $\Delta\mathbf{f} = \underline{\underline{\mathcal{K}}} \cdot \Delta\vec{\mathcal{U}}$ with dN_c-dimensional vectors, and $\underline{\underline{\mathcal{K}}}$ a *contact stiffness matrix*. $\underline{\underline{\mathcal{K}}}$ does not couple different contacts, is diagonal ($\underline{\underline{\mathcal{K}}}^E$) in elastic case (approximation).

As $\Delta\vec{\mathcal{U}} = \underline{\underline{G}} \cdot \Delta\mathbf{U}$ and $\Delta\mathbf{F}^{\text{ext}} = {}^{\mathbf{T}}\underline{\underline{\mathbf{G}}} \cdot \Delta\mathbf{f}$, (with the rigidity matrix and its transpose) one has

$$\Delta\mathbf{F}^{\text{ext}} = \underline{\underline{\mathbf{K}}}^{(1)} \cdot \Delta\mathbf{U}, \quad \text{with} \quad \boxed{\underline{\underline{\mathbf{K}}}^{(1)} = {}^{\mathbf{T}}\underline{\underline{\mathbf{G}}} \cdot \underline{\underline{\mathcal{K}}} \cdot \underline{\underline{G}}}$$

$\underline{\underline{\mathbf{K}}}^{(1)}$= $N_f \times N_f$ matrix = (structural) stiffness matrix (a.k.a. dynamical matrix) $\underline{\underline{\mathbf{K}}}^{(1)}$ symmetric if $\underline{\underline{\mathcal{K}}}$ is symmetric. Elastic form $\underline{\underline{\mathcal{K}}}^E$ $\Rightarrow$positive elements on diagonal only $\Rightarrow$ Ker $\left(\underline{\underline{\mathbf{K}}}^{(1)}\right)$ = Ker $\left(\underline{\underline{G}}\right)$.

The geometric stiffness matrix

As grains move $\mathbf{F}^{\text{int}} = -\underline{\underline{G}} \cdot \mathbf{f}$ changes because

1. contacts deform, $\vec{\mathcal{U}}$ changes, whence stiffness matrix $\underline{\underline{\mathbf{K}}}^{(1)}$
2. the direction of $\mathbf{f}$ changes, whence additional contribution $\underline{\underline{\mathbf{K}}}^{(2)}$ to stiffness matrix

$\underline{\underline{\mathbf{K}}}^{(2)}$ is not symmetric, involves radii of curvature of contacting surfaces
(general expressions written by Kuhn & Chang, and Bagi)
$\underline{\underline{\mathbf{K}}}^{(2)} \cdot \mathbf{U}$ expresses transport of force in rigid body motion, rolling, pivoting

In decomposition of stiffness matrix as

$$\underline{\underline{\mathbf{K}}} = \underline{\underline{\mathbf{K}}}^{(1)} + \underline{\underline{\mathbf{K}}}^{(2)} = {}^{\mathbf{T}}\underline{\underline{\mathbf{G}}} \cdot \underline{\underline{\mathcal{K}}} \cdot \underline{\underline{G}} + \underline{\underline{\mathbf{K}}}^{(2)}$$

$\underline{\underline{\mathcal{K}}}$ contains contact law (material behaviour + surface properties + geometry)
$\underline{\underline{G}}$ contains network geometry (normal vectors $\mathbf{n}_{ij}$ + branch vectors $\mathbf{R}_{ij}$)
$\underline{\underline{\mathbf{K}}}^{(2)}$ contains surface curvatures

The geometric stiffness matrix in the case of spheres

Normal force $F_{ij}^N \mathbf{n}_{ij}$ between 2 spheres follows motion of $\mathbf{n}_{ij}$, ($r_{ij} = ||\mathbf{r}_j - \mathbf{r}_i||$)

$$\Delta \mathbf{n}_{ij} = \frac{1}{r_{ij}} \left(\underline{\underline{1}} - \mathbf{n}_{ij} \otimes \mathbf{n}_{ij} \right) \cdot (\Delta \mathbf{u}_j - \Delta \mathbf{u}_i) \, .$$

$\mathbf{F}_{ij}^T$ follows rolling motion of $\mathbf{n}_{ij}$ and average pivoting motion of the grains.

$$\Delta \mathbf{F}_{ij}^{T\,(2)} = - \left[\mathbf{F}_{ij}^T \cdot (\Delta \mathbf{u}_i - \Delta \mathbf{u}_j) \right] \frac{\mathbf{n}_{ij}}{r_{ij}} + \frac{1}{2} \left[\left(\Delta \vec{\theta}_i + \Delta \vec{\theta}_j \right) \cdot \mathbf{n}_{ij} \right] (\mathbf{n}_{ij} \times \mathbf{F}_{ij}^T)$$

(to be added to effect of contact law).

In general (not for spheres only) one has: $K_{\alpha\beta}^{(2)} \ll K_{\alpha\beta}^{(1)}$ like $\dfrac{||\mathbf{f}||}{R} \ll K_N$.

$\Rightarrow$ Geometric matrix usually negligible, except for $\mathbf{U}$ such that $\underline{\underline{\mathbf{K}}}^{(1)} \cdot \mathbf{U} \simeq 0$

Stiffness matrix and stability

Stability criterion: one should have ($\underline{\underline{\mathbf{K}}}$ depending on $\dfrac{\Delta\mathbf{U}}{||\Delta\mathbf{U}||}$)

$$\Delta\mathbf{U}\cdot\underline{\underline{\mathbf{K}}}\cdot\Delta\mathbf{U}>0,$$

for all $\Delta\mathbf{U}$, or $\delta^2W=\Delta\mathbf{F}^{\text{ext}}\cdot\Delta\mathbf{U}>0$ (second order work).
With $\delta^2W(\mathbf{V})<0$, if grains are "kicked" in motion with velocity $\mathbf{V}$, then, at short time t, the net force

$$\Delta\mathbf{F}^{\text{int}}=-\underline{\underline{\mathbf{K}}}\cdot\mathbf{V}t$$

accelerates the motion and kinetic energy increases.

With frictionless spheres (all rotations ignored) $\underline{\underline{\mathbf{K}}}^{(2)}$ is symmetric (but *negative*)

$$a\underline{\underline{\mathbf{K}}}^{(2)}_{ij}=\frac{\mathbf{F}^N_{ij}}{r_{ij}}\left(\underline{\mathbf{1}}-\mathbf{n}_{ij}\otimes\mathbf{n}_{ij}\right)\text{ if }j\neq i,\text{ and }\underline{\underline{\mathbf{K}}}^{(2)}_{ii}=-\sum_{j\neq i}\underline{\underline{\mathbf{K}}}^{(2)}_{ij}$$

Thus mechanisms lead to instabilities if $\mathbf{F}^N_{ij}>0$, i.e. on the *backbone*, whence no displacement indeterminacy, as announced.
With friction, $\underline{\underline{\mathbf{K}}}^{(2)}\cdot\mathbf{V}=0$ for the free motion of a sphere with 2 (fixed) contacts

Computation of elastic moduli in simulations

Neglect $\underline{\underline{\mathbf{K}}}^{(2)}$, forbid free motion of 2-coordinated grains, use approximation $\underline{\underline{\mathcal{K}}} = \underline{\underline{\mathcal{K}}}^{E} \Rightarrow$ positive definite stiffness matrix $\underline{\underline{\mathbf{K}}}$, such that

$$W(\mathbf{U}) = \frac{1}{2}\mathbf{U} \cdot \underline{\underline{\mathbf{K}}} \cdot \mathbf{U}$$

is an elastic energy.

"Experimental" observation (from simulations!): in well-equilibrated states $||\mathbf{F}_T|| < \mu F_N$, whence $\underline{\underline{\mathcal{K}}} = \underline{\underline{\mathcal{K}}}^{E}$

Computation of elastic moduli in simulations (periodic boundaries)

Periodic boundaries suppress wall effects (macroscopic limit approached faster).
Define (for instance)

$$\mathbf{U} = \left((\tilde{\mathbf{u}}_i, \vec{\theta}_i)_{1 \le i \le N}, \underline{\underline{\epsilon}} \right) \quad \text{and} \quad \mathbf{F}^{\text{ext}} = \left((\mathbf{F}_i^{\text{ext}}, \mathbf{\Gamma}_i^{\text{ext}})_{1 \le i \le N}, \Omega \underline{\underline{\sigma}} \right)$$

with $\underline{\underline{\epsilon}} = \begin{bmatrix} \epsilon_1 & 0 & 0 \\ 0 & \epsilon_2 & 0 \\ 0 & 0 & \epsilon_3 \end{bmatrix}$ (or full matrix...), $\Delta\underline{\underline{\sigma}} = \begin{bmatrix} \Delta\sigma_1 & 0 & 0 \\ 0 & \Delta\sigma_2 & 0 \\ 0 & 0 & \Delta\sigma_3 \end{bmatrix}$, and $\tilde{\mathbf{u}}_i$ the (periodic) displacements superimposed on global strain effects, so that

$$\mathbf{u}_i = -\underline{\underline{\epsilon}} \cdot \mathbf{r}_i + \tilde{\mathbf{u}}_i \; = \; \text{displacement of } i$$

Computation of elastic moduli in simulations (periodic boundary conditions)

Relative displacements (definition of $\underline{\underline{G}}$) involve $\mathbf{r}_{ij} = \mathbf{r}_j - \mathbf{r}_i$ (with nearest image convention):

$$\vec{\mathcal{U}}_{ij} = \tilde{\mathbf{u}}_i - \tilde{\mathbf{u}}_j + \underline{\underline{\epsilon}} \cdot \mathbf{r}_{ij}.$$

Then solve

$$\Delta \mathbf{F}^{\text{ext}} = \left(\mathbf{0}, \mathbf{0}\right)_{1 \leq i \leq N}, \Delta \underline{\underline{\sigma}}\right) = \underline{\underline{\mathbf{K}}} \cdot \mathbf{U}$$

for unknown $\mathbf{U}$ (which comprises $\underline{\underline{\epsilon}}$), and deduce compliances. Alternatively, impose $\underline{\underline{\epsilon}}$ fixed, and use

$$\begin{bmatrix} \underline{\underline{\tilde{\mathbf{K}}}} & \underline{\underline{\mathbf{L}}} \\ {}^{\mathbf{T}}\underline{\underline{\mathbf{L}}} & \underline{\underline{\mathbf{k}}} \end{bmatrix} \cdot \begin{bmatrix} \mathbf{U}_1 \\ \underline{\underline{\epsilon}} \end{bmatrix} = \begin{bmatrix} \mathbf{0} \\ \Delta \underline{\underline{\sigma}} \end{bmatrix} \Rightarrow \underline{\underline{\tilde{\mathbf{K}}}} \cdot \mathbf{U}_1 = -\underline{\underline{\mathbf{L}}} \cdot \underline{\underline{\epsilon}}$$

Elastic moduli might also be directly computed by standard DEM, imposing small strain or stress increments in various directions (costlier, but also yields elastic range)

Estimation of elastic moduli (isotropic case)

Naive Voigt approach $\tilde{\mathbf{u}}_i = 0$ into formula for $\underline{\underline{\sigma}}$, to be evaluated as sums (talk2) over contacts, results in

$$B^{\text{Voigt}} = \frac{z\Phi}{3\pi}\langle K_N \rangle = \frac{Z(1/3)}{2}\left(\frac{z\Phi\tilde{E}}{3\pi}\right)^{2/3} P^{1/3}; \quad G^{\text{Voigt}} = \frac{6+9\alpha_T}{10} B^{\text{Voigt}},$$

with $\alpha_T = \dfrac{K_T}{K_N} = \dfrac{2-2\nu}{2-\nu}$.

Uses $\langle K_N f(\mathbf{n}_{ij}) \rangle = \langle K_N \rangle f(\mathbf{n}_{ij})$, values of $\langle (n_{ij}^x)^4 \rangle$, etc...

Estimation of elastic moduli (isotropic case) : variational approach I

If $\mathbf{F}^{\text{ext}}$ is imposed $\mathbf{U}$ minimizes

$$W_1(\mathbf{U}) = \frac{1}{2}\mathbf{U} \cdot \underline{\underline{\mathbf{K}}} \cdot \mathbf{U} - \Delta\mathbf{F}^{\text{ext}} \cdot \mathbf{U},$$

Find best value of $\underline{\underline{\epsilon}}$ for trial $\mathbf{U}$ with $\tilde{\mathbf{u}}_i = 0$ and $\vec{\theta}_i = 0$ for all i.
Impose $\Delta\sigma_1 = \Delta\sigma_2 = \Delta\sigma_3 = \Delta P \Rightarrow$ optimal value $W_1^* = -\frac{\Omega}{3B}(\Delta P)^2 \Rightarrow$ *upper bound to* B

With $\Delta\sigma_1 = -\Delta\sigma_2 = q$, $\Delta\sigma_3 = 0$, optimal value = $W_1^* = -\frac{\Omega}{2G}q^2 \Rightarrow$ *upper bound to* G

Results identical to "naive Voigt approach", but shows B^{Voigt} and G^{Voigt} are estimates *in excess* of true moduli

Estimation of elastic moduli (isotropic case): variational approach II

Increments of contact forces $\Delta\mathbf{f}$ minimize

$$W_2(\Delta\mathbf{f}) = \frac{1}{2}\Delta\mathbf{f}\cdot\underline{\underline{\mathcal{K}}}^{-1}\cdot\Delta\mathbf{f}$$

under the constraint that they balance applied load increment $\Delta\mathbf{F}^{\text{ext}}$,

$$^{\mathbf{T}}\underline{\underline{\mathbf{G}}}\cdot\Delta\mathbf{f} = \Delta\mathbf{F}^{\text{ext}}.$$

With increment of pressure, optimal value $W_2^* = \frac{\Omega}{3B}(\Delta P)^2$, $W_2^* = \frac{\Omega}{2G}q^2$ with deviator $q \Rightarrow$ *lower bounds to* B *and* G

Note importance of force indeterminacy. Trial $\Delta\mathbf{f}$? Available choice for ΔP under isotropic pressure P:

Choose $\Delta\mathbf{f} = \dfrac{\Delta P}{P}\mathbf{f}$!

Defining $\tilde{Z}(5/3) = \langle F_N^{5/3}\left(1+\frac{5r_{TN}^2}{6\alpha_T}\right)\rangle/\langle F_N\rangle^{5/3}$, with $r_{TN} = \frac{||\mathbf{F}_T||}{F_N}$ ($\tilde{Z}(5/3)$ only slightly larger than $Z(5/3)$),

$$B \geq B^{\text{Reuss}} = \frac{z\Phi}{3\pi}\langle K_N\rangle = \frac{1}{2\tilde{Z}(5/3)}\left(\frac{z\Phi\tilde{E}}{3\pi}\right)^{2/3}P^{1/3}$$

Estimation of bulk modulus in isotropic states

With $B^e = \frac{1}{2}\left(\frac{z\Phi\tilde{E}}{3\pi}\right)^{2/3} P^{1/3}$

$$\boxed{\frac{B^e}{\tilde{Z}(5/3)} = B^{\text{Reuss}} \leq B \leq B^{\text{Voigt}} = Z(1/3)B^e}$$

- The smaller the degree of force indeterminacy, the better the "Reuss" approximation
- Note rather accurate bracketing of B (response to stress increment proportional to previous stress). $Z(1/3)\tilde{Z}(5/3) \geq Z(1/3)Z(5/3) \geq 1$ always satisfied.
- No such lower bound for G
- Ratio G/B estimated at $(6+9\alpha_T)/10 \simeq 1.34$ (with $\nu = 0.3$ for glass), whence a very small effective Poisson ratio $\nu^* \simeq 0.03$
- more elaborate schemes available (L. La Ragione, J. Jenkins 2007 = LRJ) $\Rightarrow$ estimates lower than Voigt ones

Elastic moduli vs. P in isotropic systems

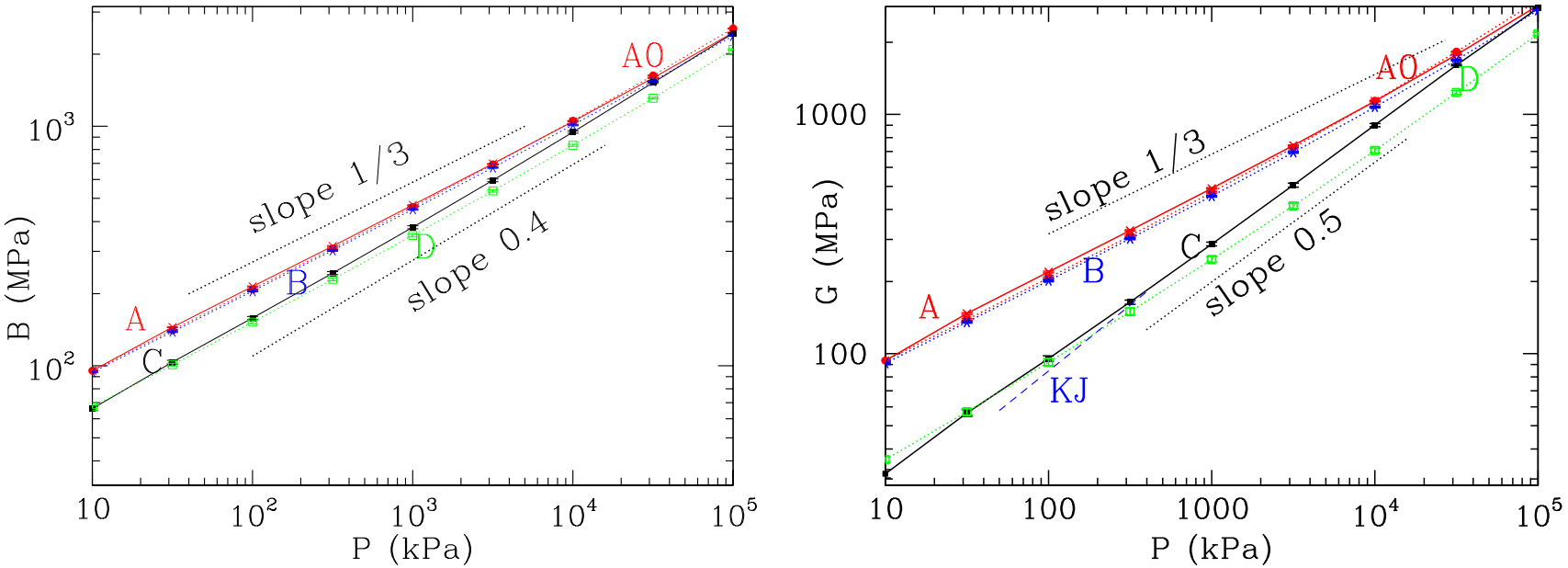

A and B : high z^* (~ 6 under low P) ; C et D : low z^* (~ 4.5)

But $\Phi_A \simeq \Phi_C > \Phi_B > \Phi_D$.

KJ = Kuwano & Jardine (2005), measurements on loose glass bead sample $\Rightarrow$ measure **moduli** to infer **coordination** number z^*?

Elastic moduli and coordination number

Plot $b_r = B/(\tilde{E}^{2/3}P^{1/3})$, $g_r = G/(\tilde{E}^{2/3}P^{1/3})$ versus $(z\Phi)^{2/3}$ for all configurations A, B, C, D in pressure *cycle*

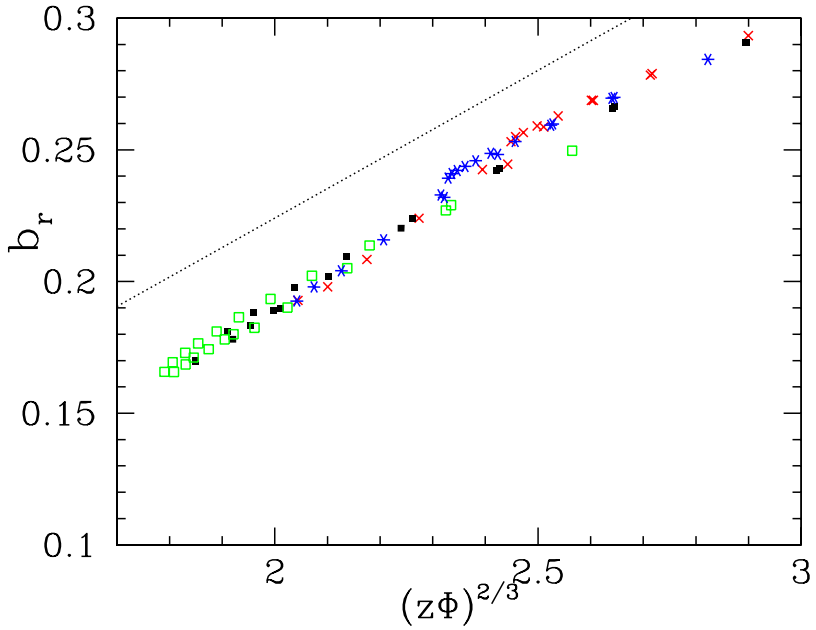

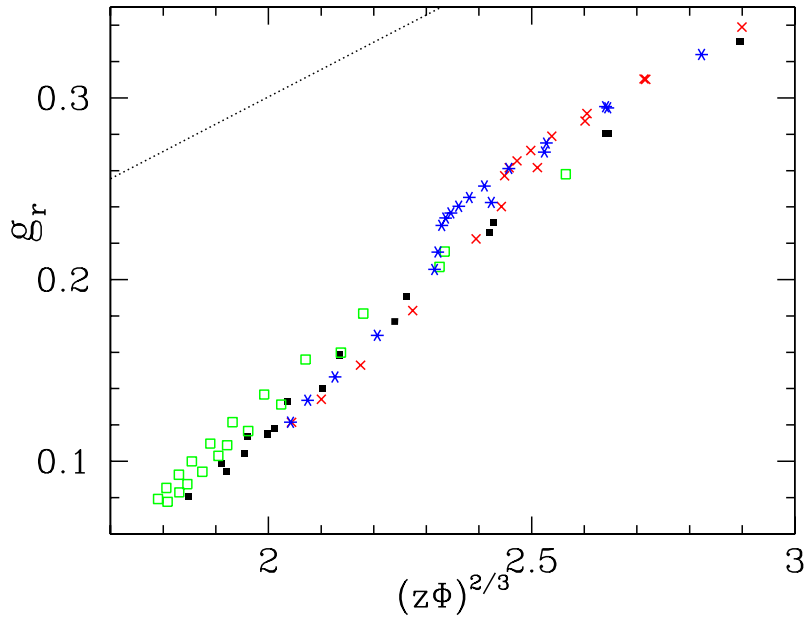

Dotted, straight lines show B^e and $G^e = \dfrac{6+9\alpha_T}{10}B^e$

Comparison with experiments: speed of sound waves

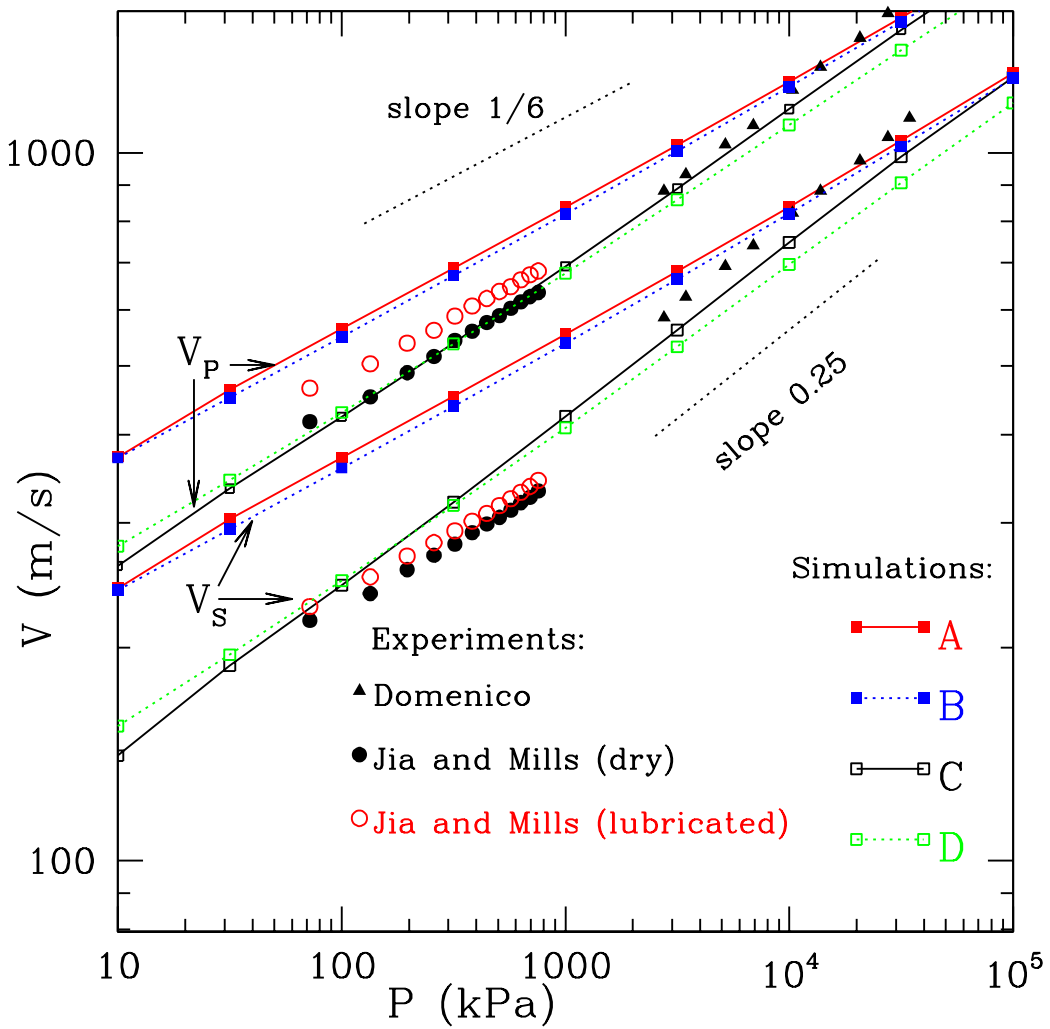

C= better model for dry grains. Effects of lubrication in the lab (Φ decreases from 0.64 to 0.62) similar to B compared to C. Anisotropy ?

Diversity of experimental results for speed V_P.

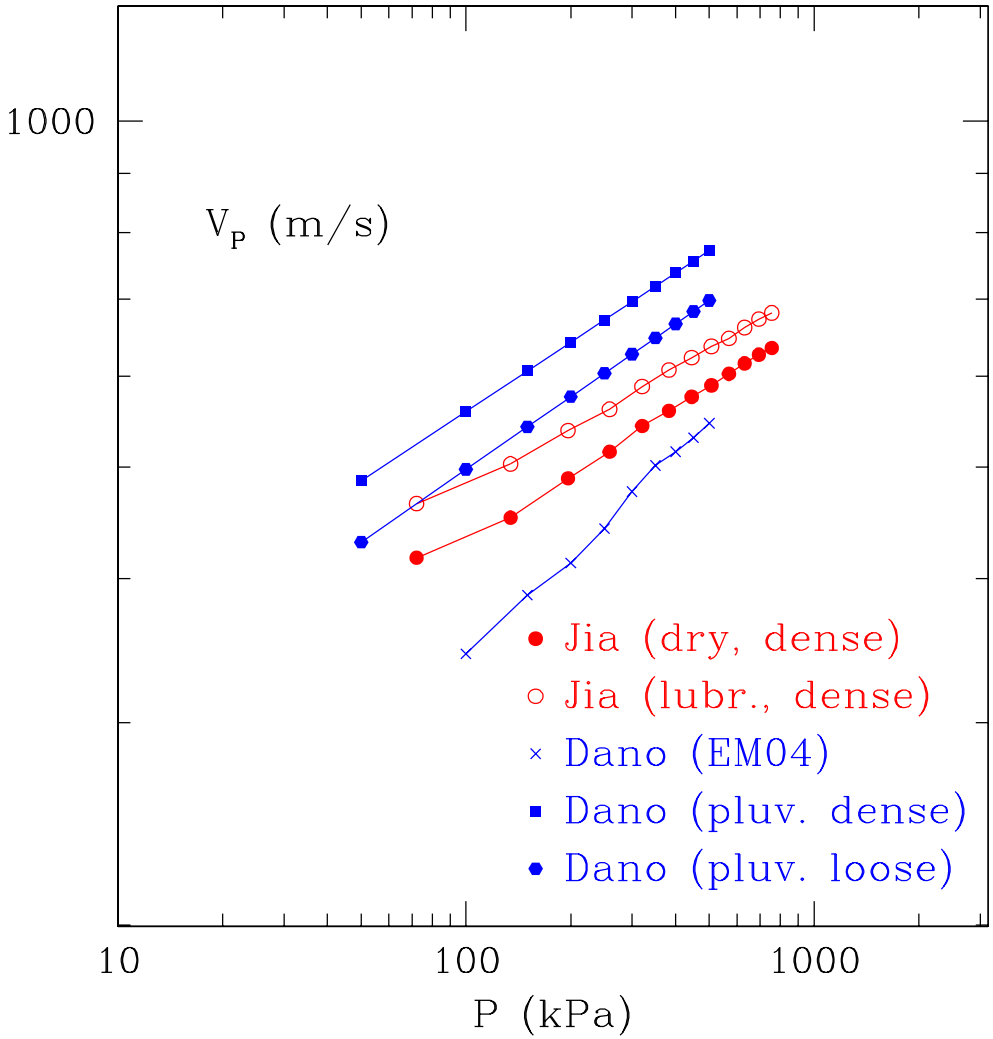

- Jia = Marne-la-Vallée
  (X. Jia, P. Mills).
  Vibration or lubrication, oedometric confinement
- Dano = results of Sharifipour, Dano, Hicher, Ecole Centrale de Nantes.
  1 vibrated sample (EM04),
  2 pluviated ones
  Isotropic pressure

Vibrated $\Rightarrow$ lower wave velocity

Numerical results for V_P (pluviation)

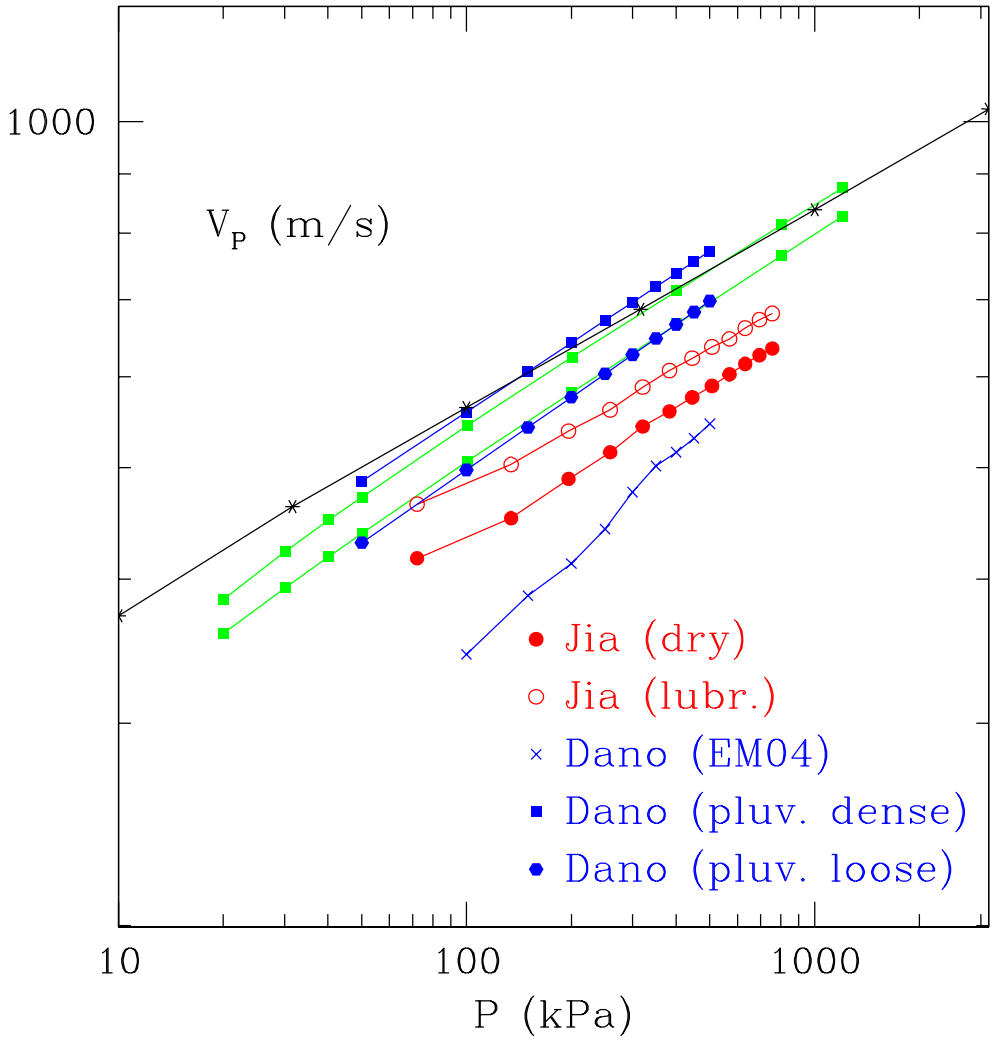

Ratio of longitudinal moduli in $\neq$ directions ~ 1.1

SIMULATIONS:

- **A : very dense, isotropic, large z (~ 6)**
- pluviation,
  $\mu = 0.3$, $\alpha_T = 0$
  $H_p^* = 0$ and $H_p^* = 20$

Numerical vs. experimental results for V_S (pluviation)

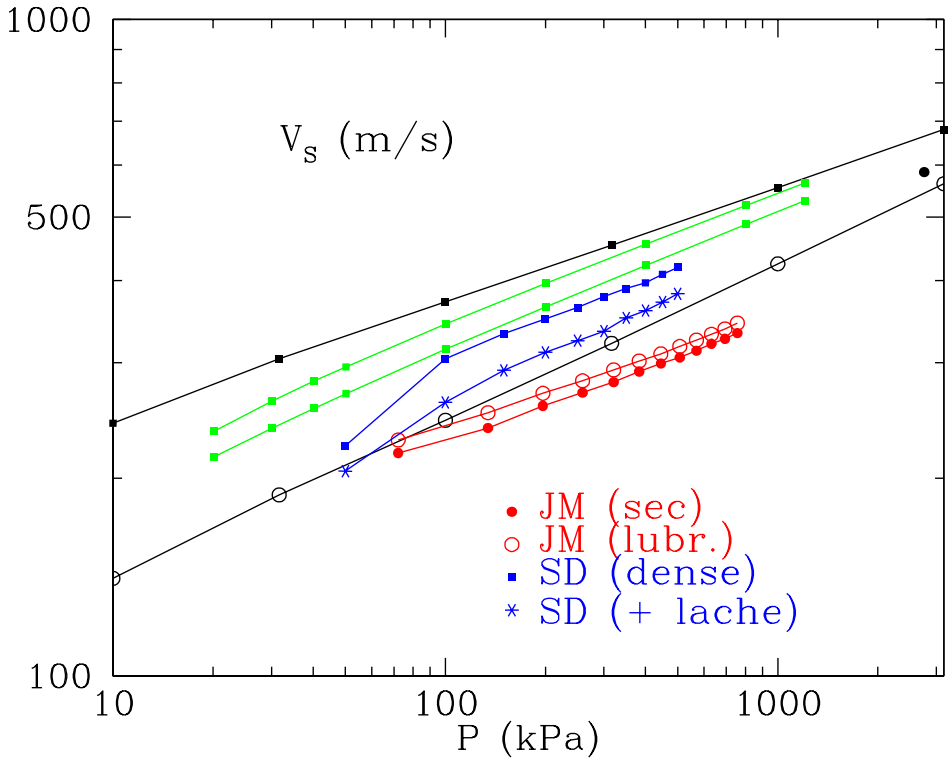

SIMULATIONS:

- **A : very dense, isotropic, large z (~ 6)**
- Open dots = dense, low coordination number (C)
- pluviation,
  $\mu = 0.3$, $\alpha_T = 0$
  $H_p^* = 0$ and $H_p^* = 20$

EXPERIMENTS: Dano *et al.*, JM=Jia-Mills as on previous slide

Not as good an agreement as for V_P !

Predictions for elastic moduli.

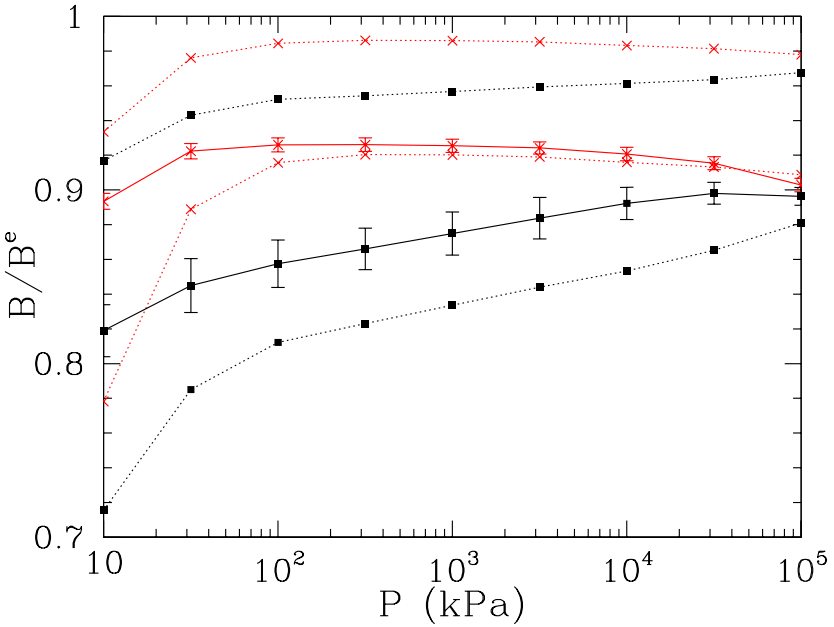

B/B^e (with error bars),
bounds $Z(1/3)$, $1/\tilde{Z}(5/3)$ for **A** and **C**

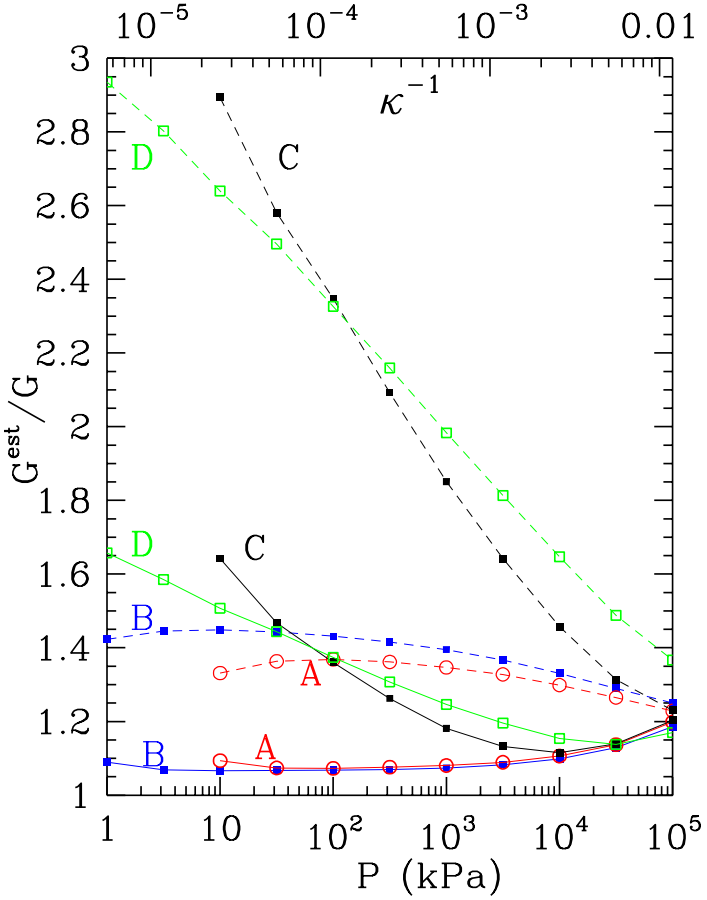

Estimations of G: G^{Voigt} (dashed lines),
G^{LRJ} (solid lines)

Systems with low degree of force indeterminacy: frictionless case

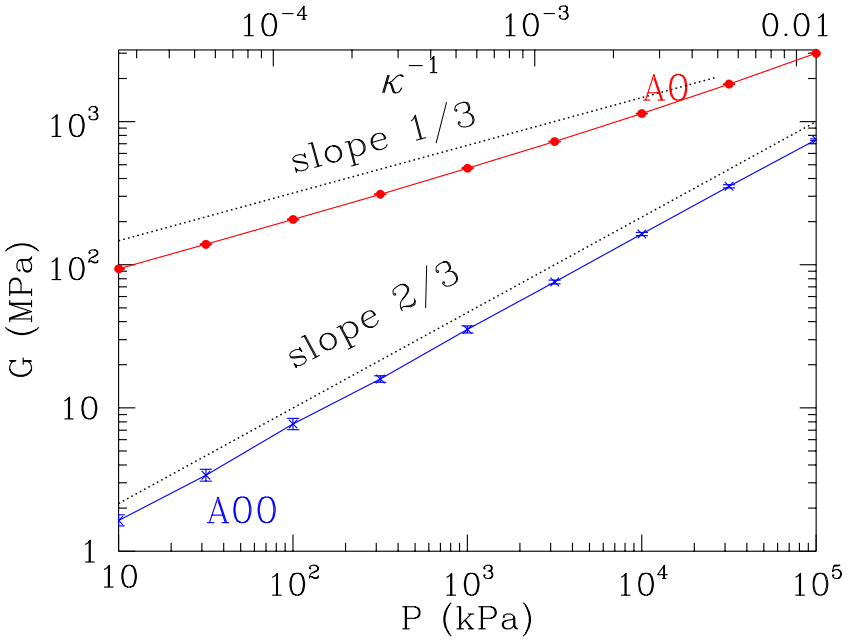

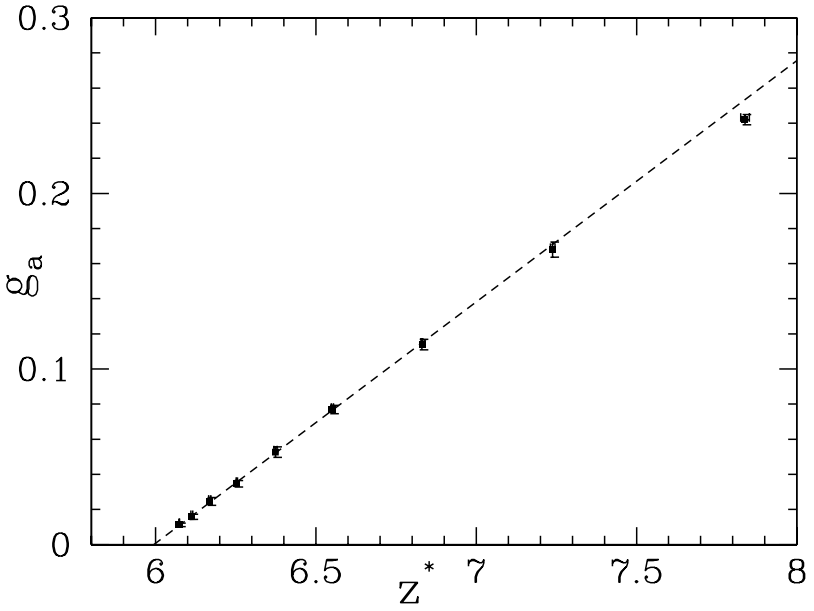

A0 = assembled and confined without friction, tangential elasticity. A00 = frictionless case.

G has anomalous scaling with pressure. g_a = singular amplitude (remove obvious factors of average stiffness, etc... defining $g_a = \frac{Gz^{1/3}}{\tilde{E}^{2/3}P^{1/3}Z(1/3)(1-x_0)\Phi^{2/3}}$),

g_a vanishes proportionnally to degree of hyperstaticity, as $z^* - 6$

Systems with low degree of force indeterminacy: frictional case

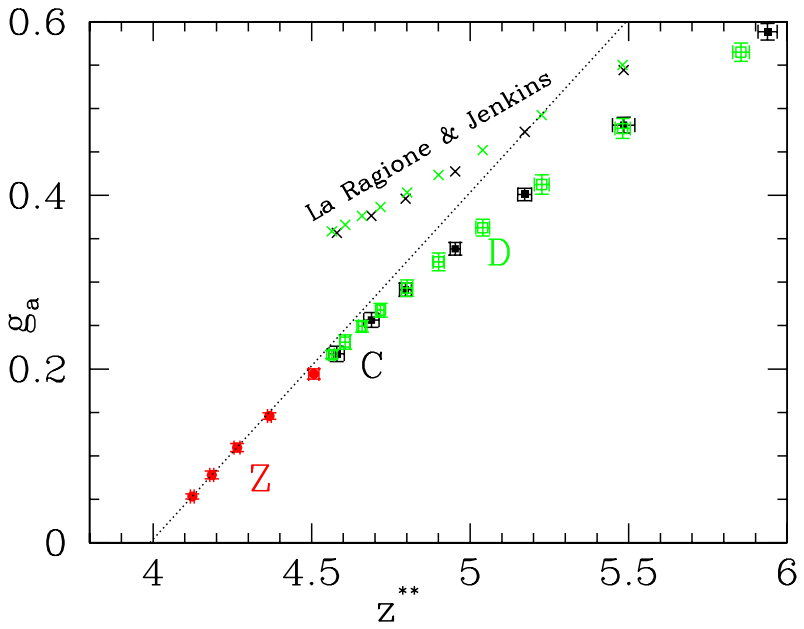

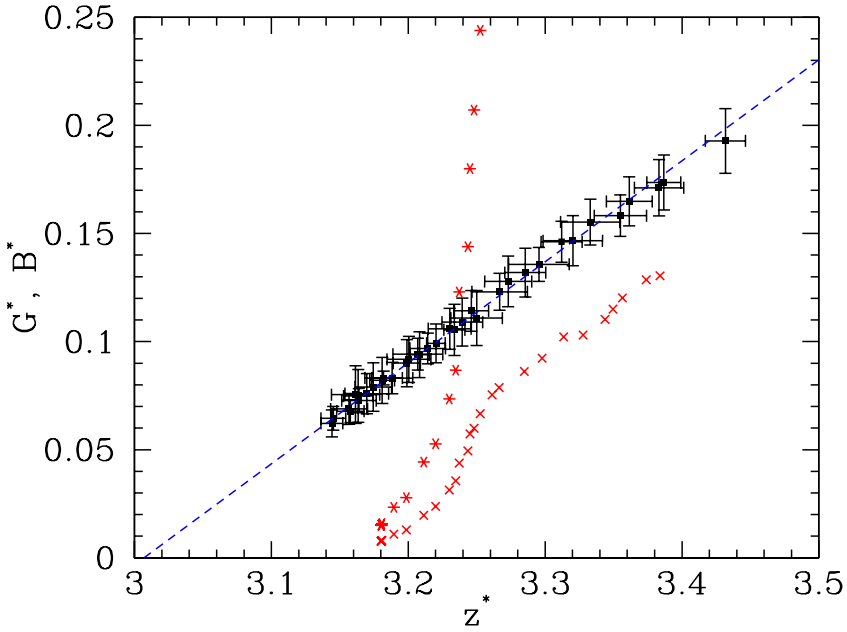

Left: low-coordinated 3D systems **C**, **D** AND **Z**, the latter assembled with $\mu = +\infty$, so that indeterminacy approaches zero.

z^{**} corrects z^* for effect of 2-coordinated grains. $z^{**} = z^* + 2x_2/[3(1-x_0)]$

Right: 2D case (see black data points)

$\Rightarrow$ Singular factor in G tends to zero proportionally to degree of hyperstaticity!

s

Systems with low degree of force indeterminacy

- Proportionality $G \propto \frac{h}{N_f}$ was proposed by M. Wyart (2005, PhD thesis, Annales de Physique)
  Argument relies on additive effects of addition of contacts to isostatic structure for shear strain energy (but not for volumetric strain!)
- Difference between B (correctly estimated, not especially singular) and G due to consideration of *isotropically prestressed* systems. In general (P.-E. Peyneau& J.-N. R., Phys Rev E 2008) distinguish response to $\Delta\underline{\underline{\sigma}}$ proportional to $\underline{\underline{\sigma}}$
- Weakly hyperstatic systems also have anomalous distribution of vibration modes (eigenvalues of stiffness matrix), with a large excess of soft ones

Conclusions

- Elastic moduli in simulated systems compare well to experimental results (although information is sometimes incomplete on available laboratory measurements)
- Predictions of moduli: possible for $\Delta\underline{\underline{\sigma}} \propto \underline{\underline{\sigma}}$, more difficult in other cases (more sophisticated schemes available)
- Systems with low coordination number have anomalous elastic properties: low G (if stresses isotropic) prop. to degree of hyperstaticity (and soft modes)
- Stiffness matrices useful in study of quasistatic anelastic response too
- Anisotropic systems assembled by controlled pluviation have moderately anisotropic moduli under isotropic pressure.
- Measurement of elastic moduli: interesting as non-destructive characterization method
  Essentially determined by coordination number.

STRESS-STRAIN BEHAVIOUR

1. Elastic regime and beyond
2. The origins of strain
3. Deformation of a contact network before its failure
4. Network rearrangements
5. Stress, strain and fabric. The critical state

Linear elastic regime and beginning of triaxial compression

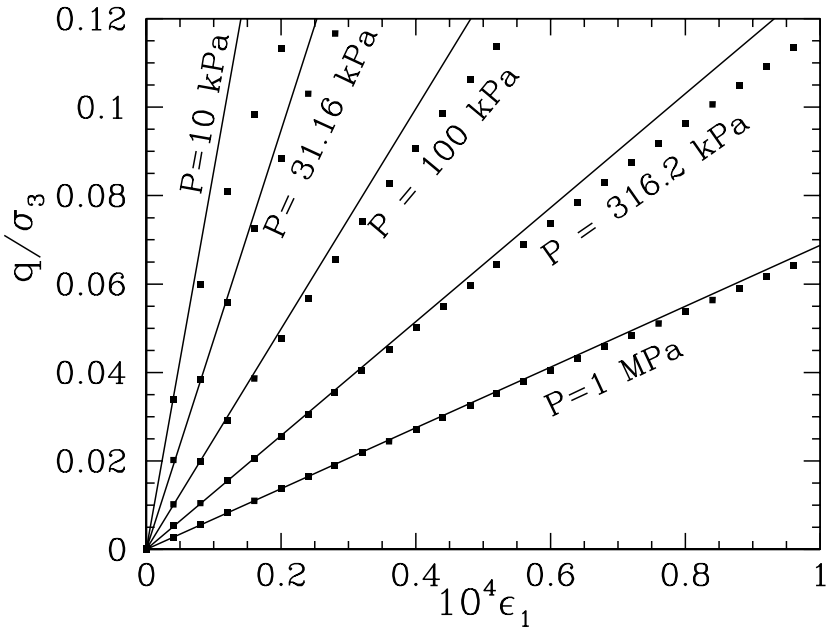

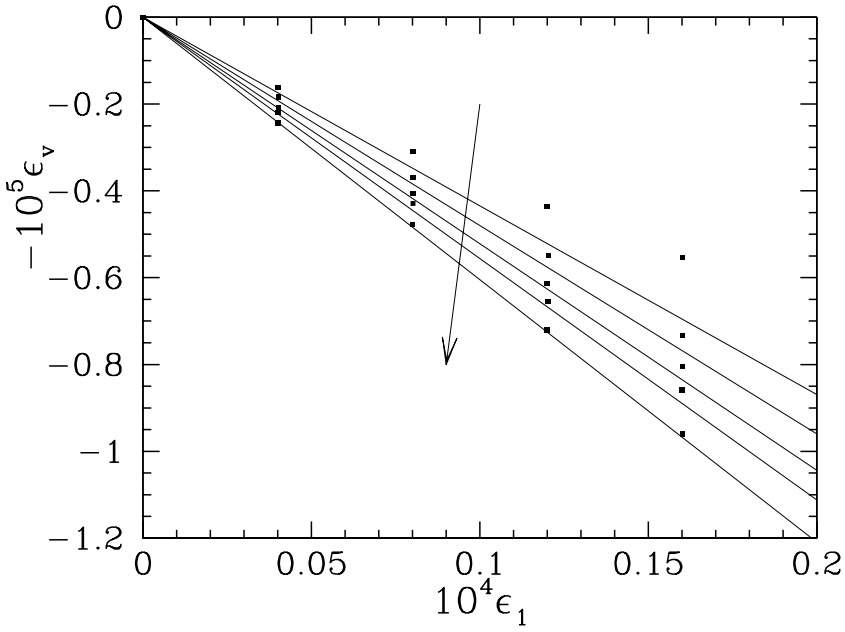

C-type sample (dense, small coordination). Triaxial compression, $q = \sigma_1 = \sigma_3$, constant $\sigma_2 = sigma_3$.

Left = q versus $\epsilon_a = \epsilon_1$, right = ϵ_v versus ϵ_a

Dots = DEM results ; Continuous line = initial slope from evaluation of moduli with stiffness matrix

Initial values of E^* and $1 - 2\nu^*$

Linear elastic range

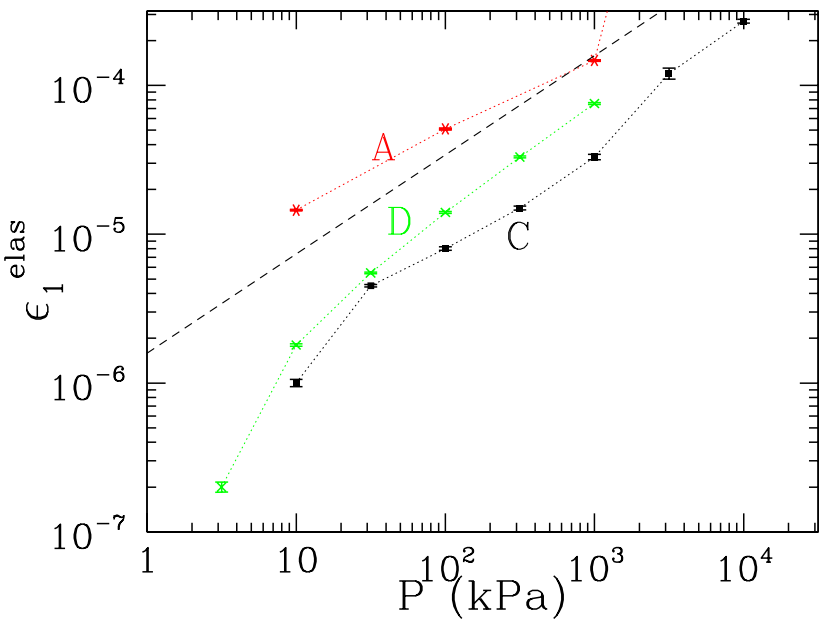

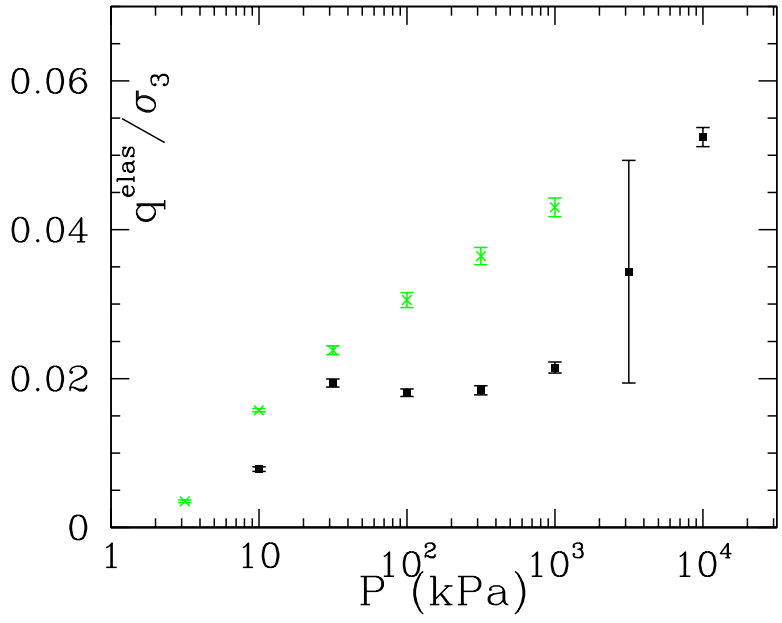

As conventionnally defined from $\dfrac{q - E^* \epsilon_a}{E^* \epsilon_a} < 0.05$.

Left: as ϵ_a interval; Dashed line has slope $2/3$

Right: as $\Delta q/q$ interval. Note smaller P dependence, larger initial state dependence

Small strains, load reversal, and initial network response

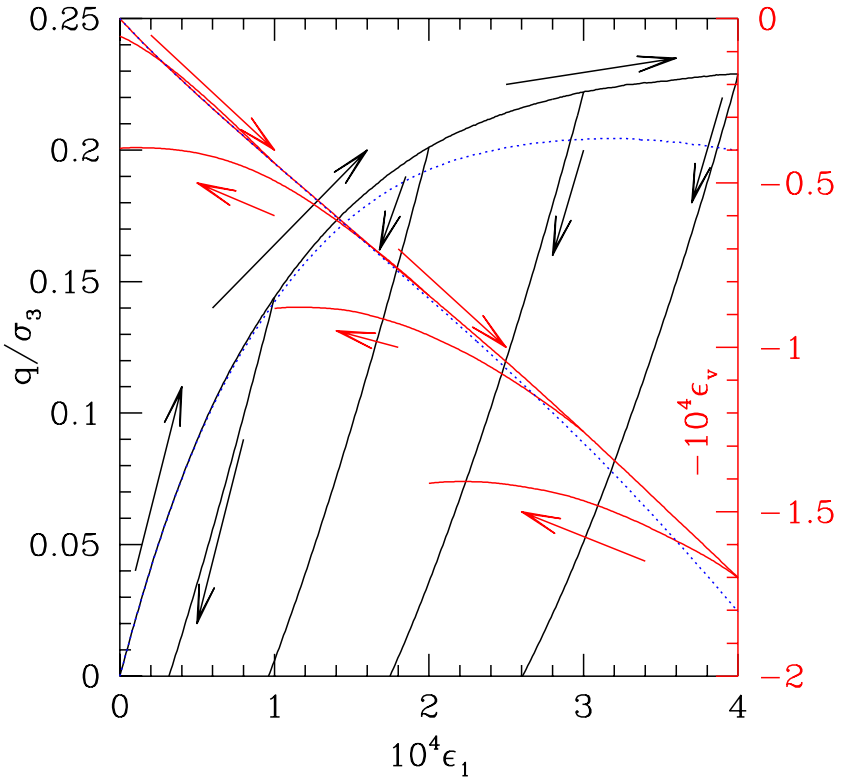

Initial state **C** (low z).

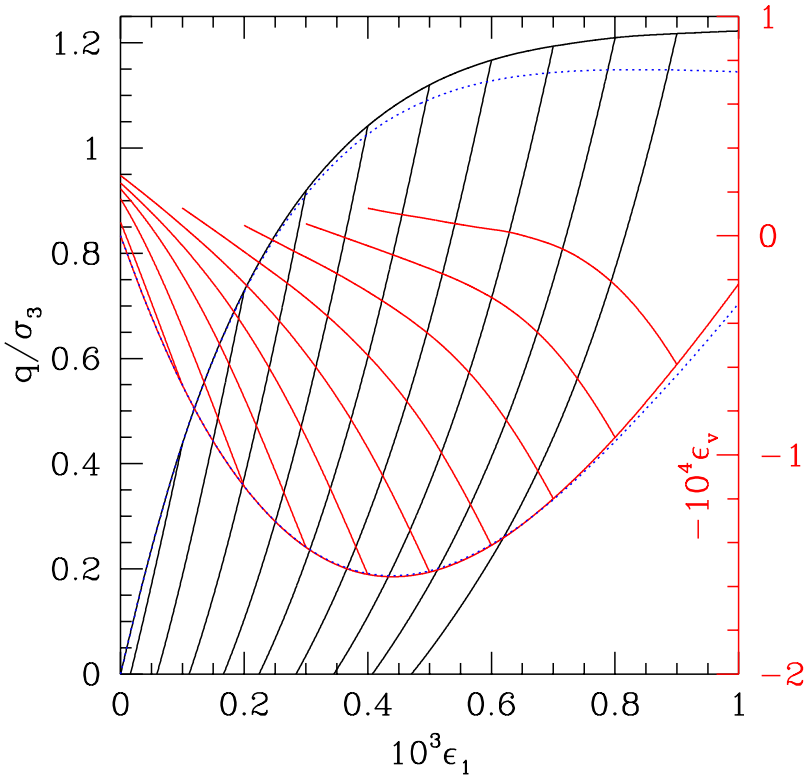

Initial state **A** (large z).

Load reversal at different stages. Elastic range = linear elastic range.

Thin blue line = computation without new contacts $\Rightarrow$ beginning of curves express response of fixed network. *Note (different) blown-up strain scales*

$\mu = 0.3$, $P_0 = \sigma_2 = \sigma_3 = 100$ kPa ($\kappa \simeq 8400$)

Comparison with isotropic compression cycle

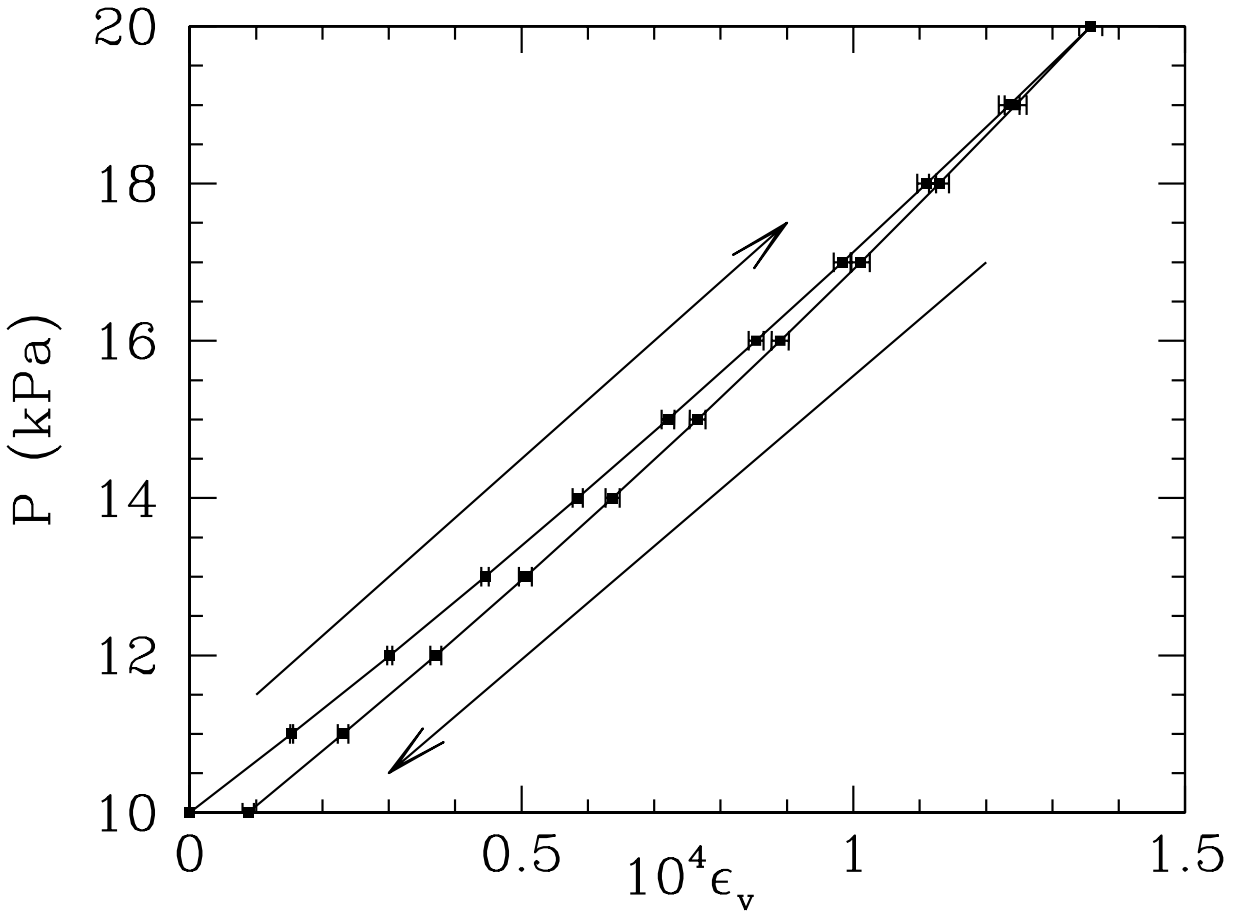

One **C** sample

Much closer to elastic for larger relative stress changes! (P $\times 2$)

Reproducibility and stress-strain curves: from initial to peak deviator state

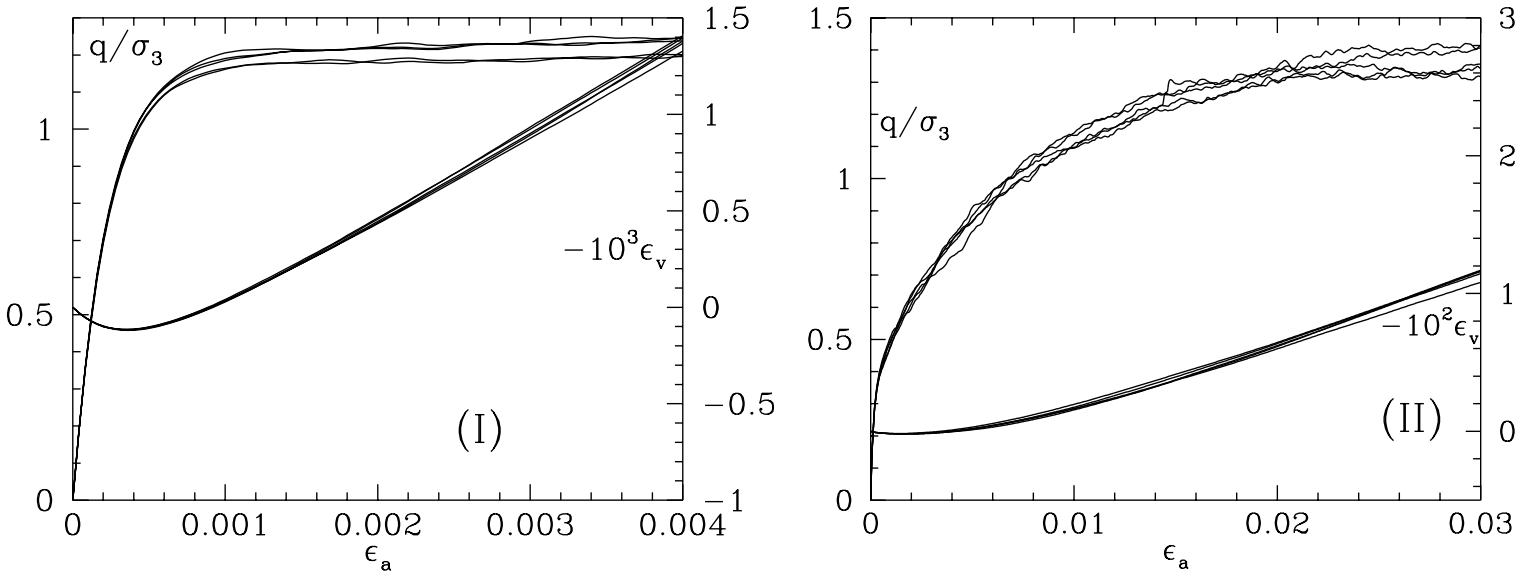

5 samples of 4000 beads. Note different strain scales in cases I = **A** and II = **C**

Lateral confining strain = 100 kPa for glass beads ($\kappa \simeq 8400$)

Peak strength apparently given by initial density and intergranular friction (for large enough κ), but strain to peak related to coordination number.

Effect of initial coordination number (for given density) and of dynamical parameters

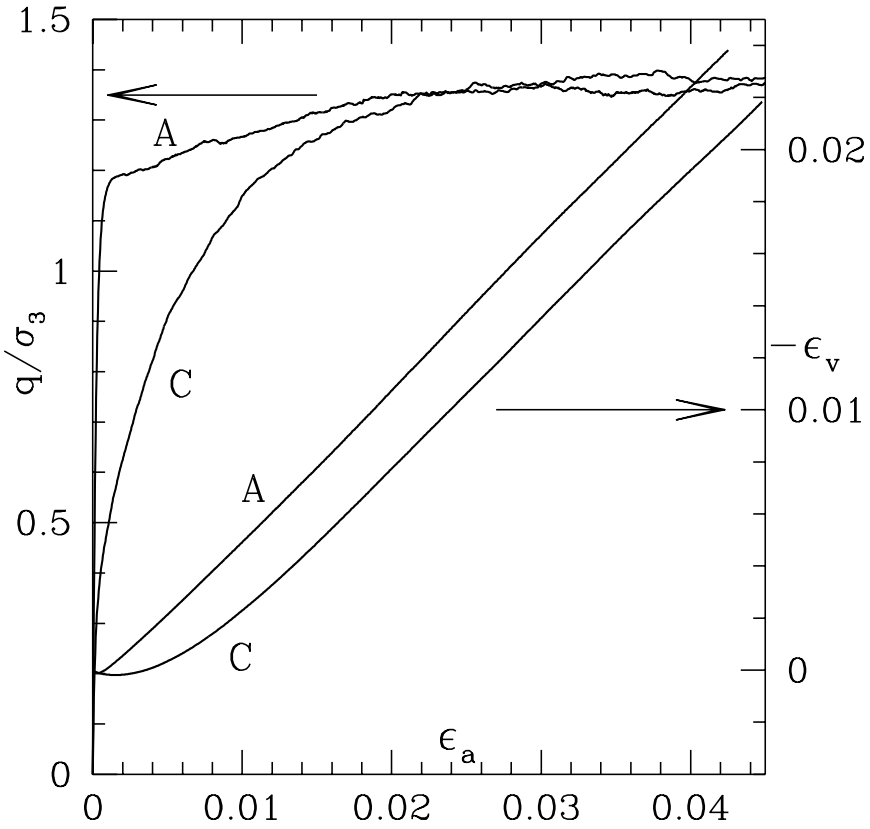

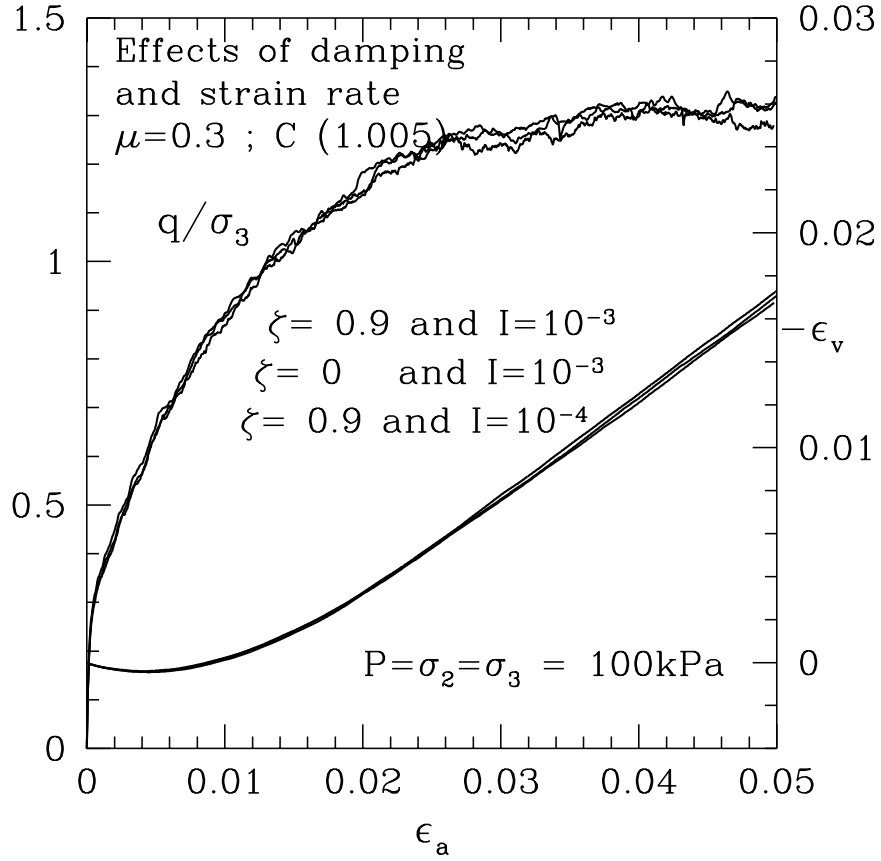

Level of damping relative to "critical" one = ζ. Inertial number $I = \dot{\epsilon}_a \sqrt{\frac{m}{aP}}$ characterizes dynamical effects

Triaxial compression, influence of κ, few contacts initially

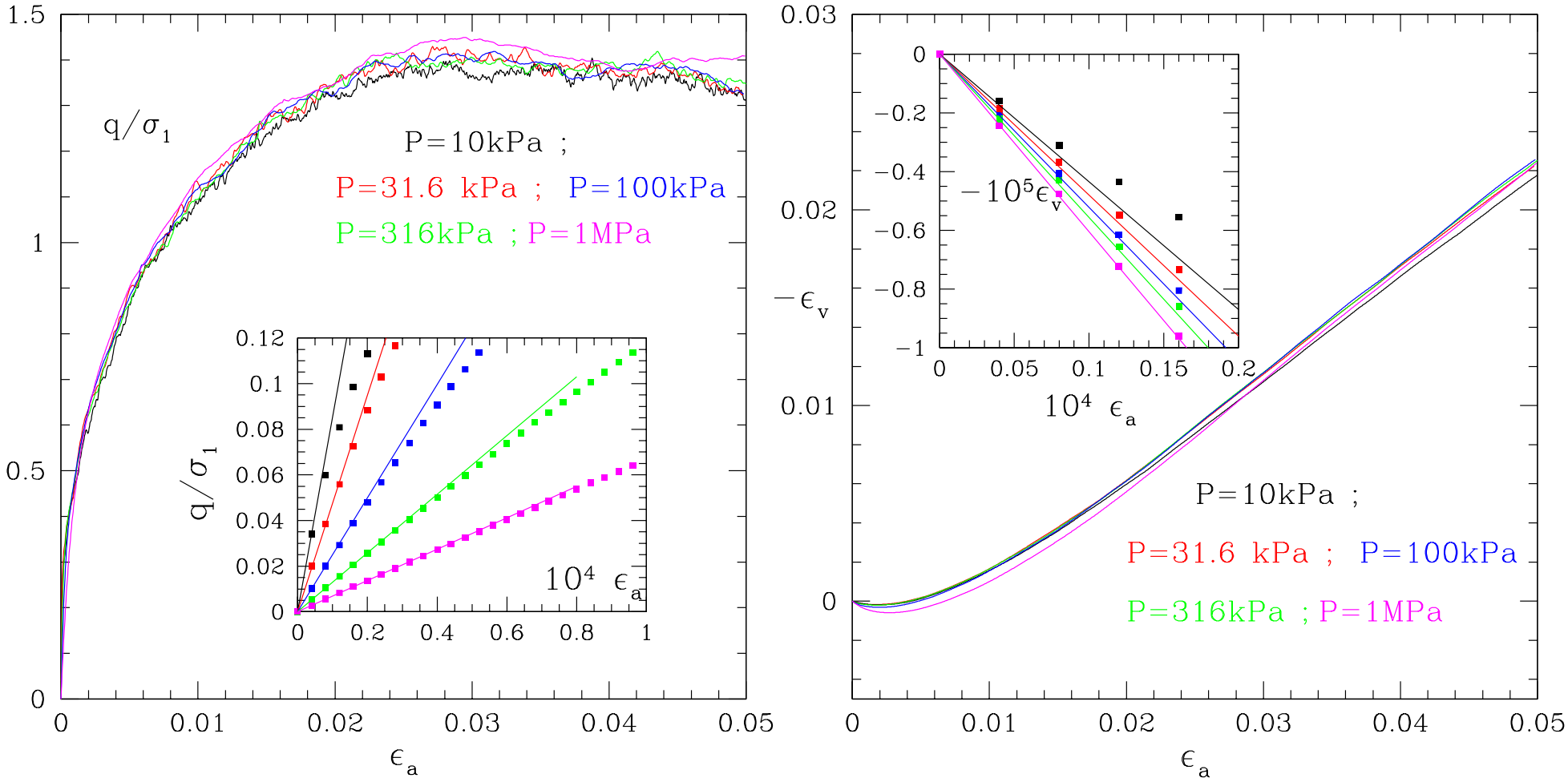

Dense state C ($\Phi \geq 0.635$ for large κ), weak $z^* \simeq 4.6$ if $\kappa \geq 10^4$ (10 kPa). Strain independent of κ except for ϵ_a very weak (slope in insert = elastic modulus)

Type II strains: contact network breaks

Triaxial compression, influence of κ, many contacts in initial state

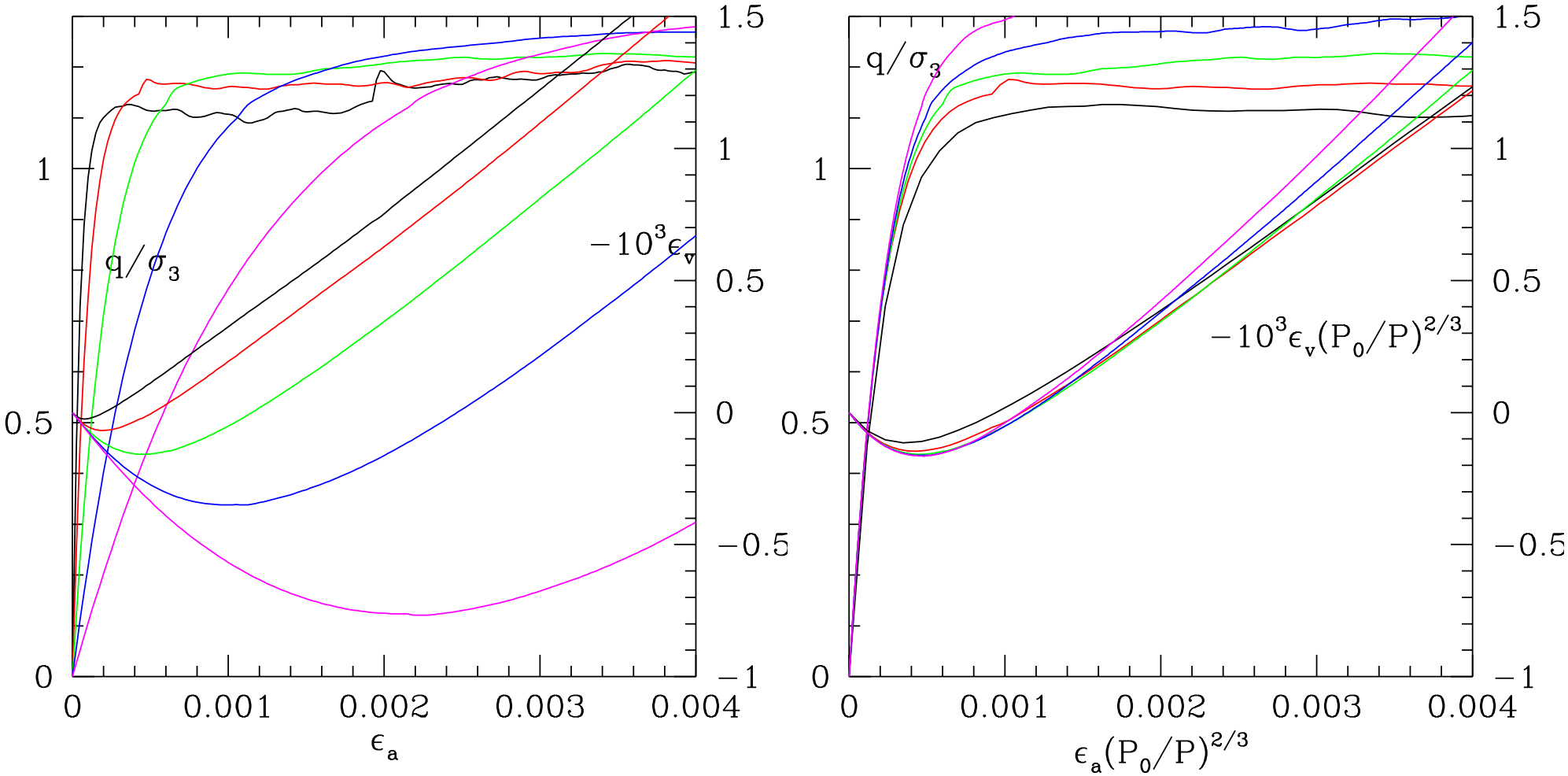

Dense state A ($\Phi \simeq 0.637$), large $z^* \simeq 6$ if $\kappa \geq 10^4$ (10 kPa). Strain of order κ^{-1}.

Type I strains: initial contact network resists

Some observations on regimes I and II

- Regime I:
  - strictly quasistatic, granular assembly behaves like network of springs and plastic sliders. Strains inversely proportional to spring constant
  - Smooth response in finite samples
  - Excludes macroscopic instabilities. Failure at some deviator value depending on initial state (coodination number/friction mobilization). Static calculation possible. Uniqueness (ignoring contact losses) if second order work criterion satisfied for all increment directions (S. McNamara).
  - Contact losses, no gains
- Regime II:
  - Contact network keeps getting broken and repaired (need for new contacts!)
  - Small simulation samples exhibit microscopic instabilities (bursts of kinetic energy), which *does not necessarily imply* macroscopic instability.

Induced anisotropy

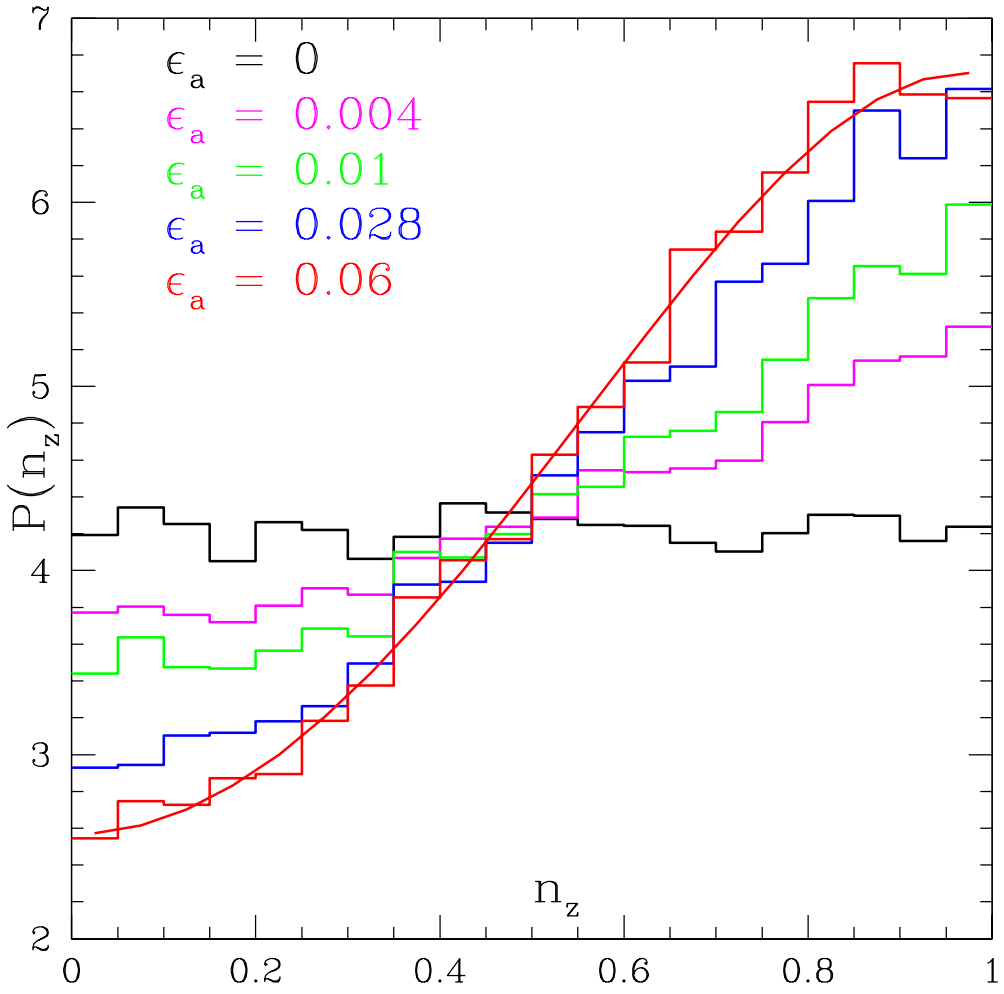

Triaxial compression of **C** sample

Observation of elastic moduli on unloading

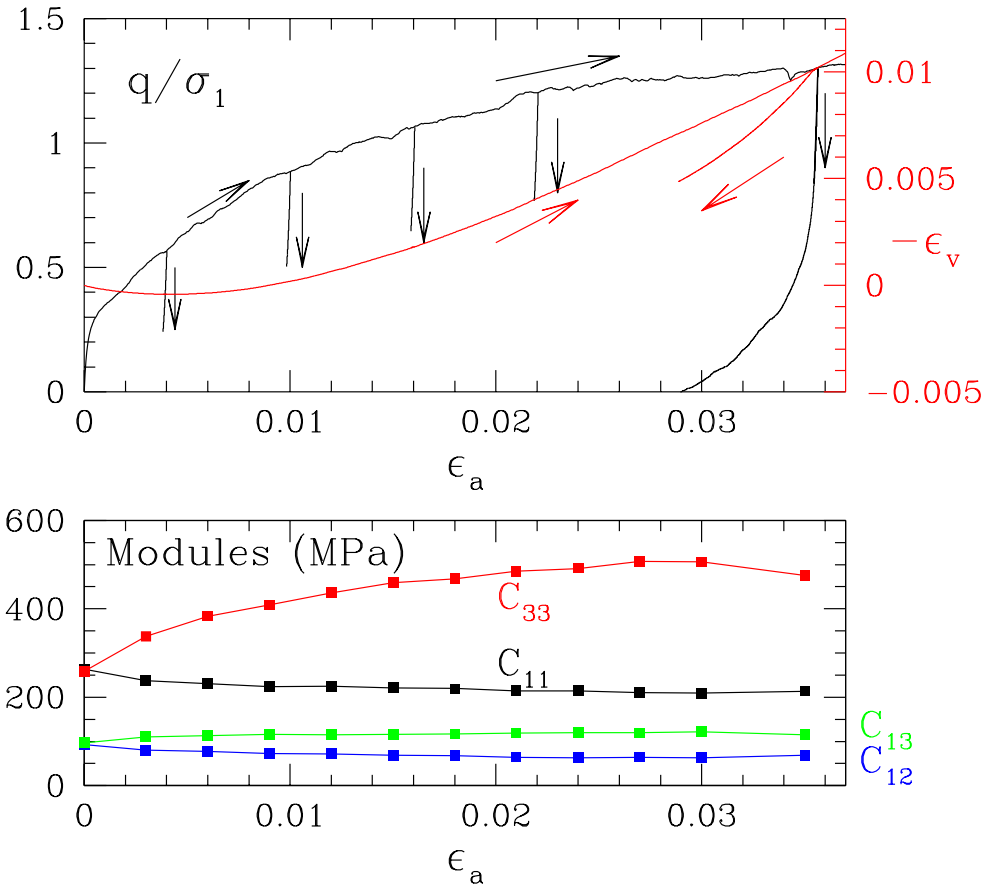

Moduli sensitive to fabric anisotropy AND to stress anisotropy

N. B. Index 3 here corresponds to vertical (major principal) compression axis, denoted with index 1 in rest of document.

Equilibration under constant stress and resumed strain-rate controlled test

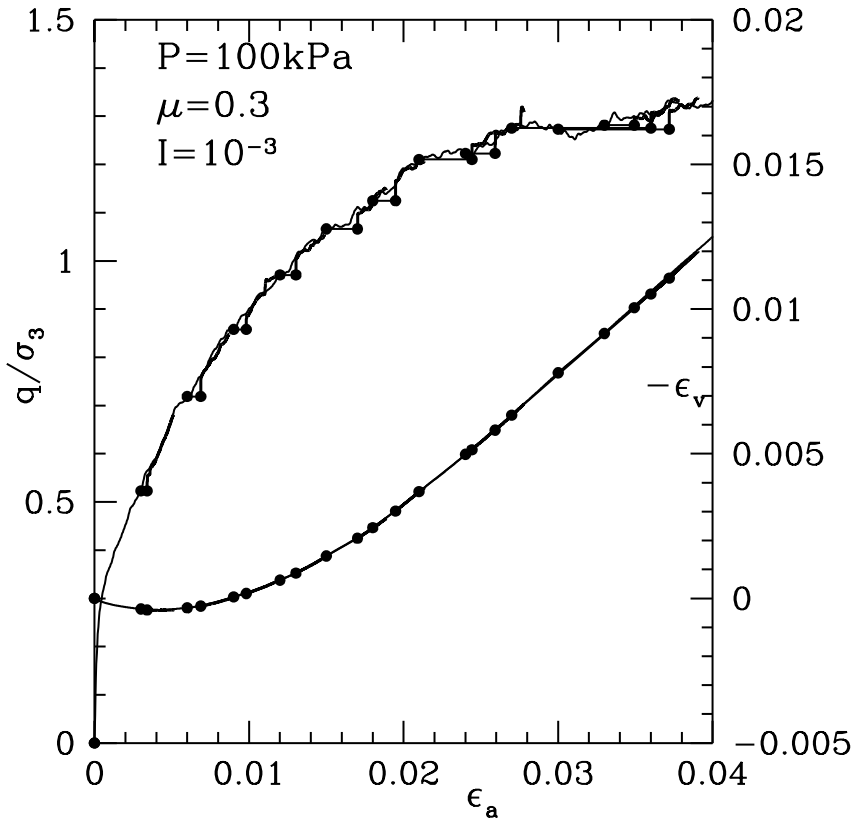

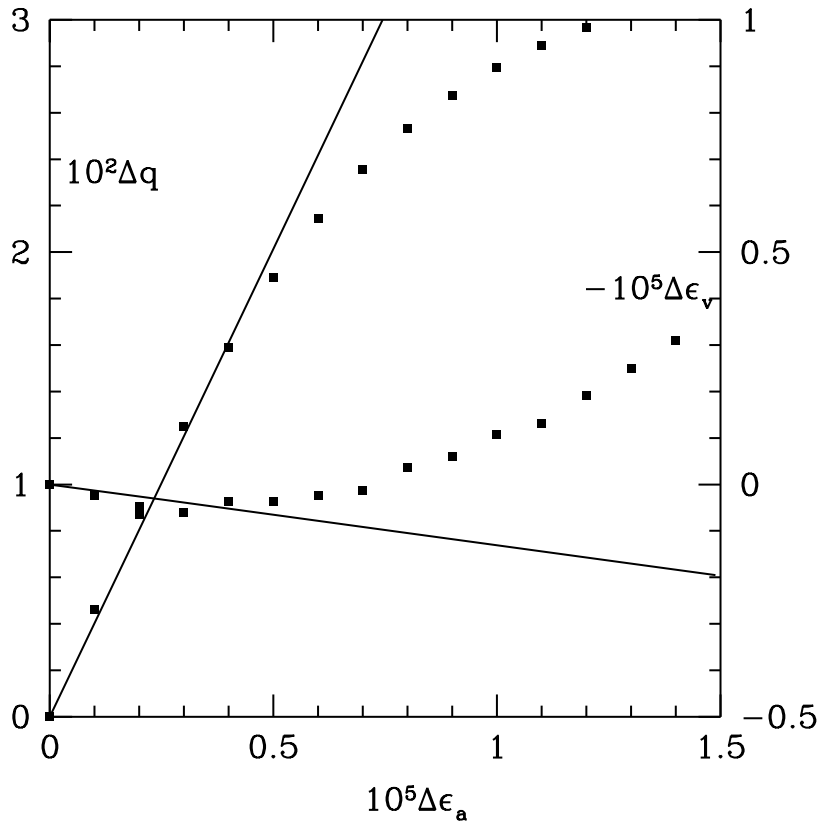

Elastic moduli (right plot) observed after test is stopped under constant stresses and some creep is observed before a well equilibrated configuration is obtained. (Reminiscent of some experimental results)

Critical state

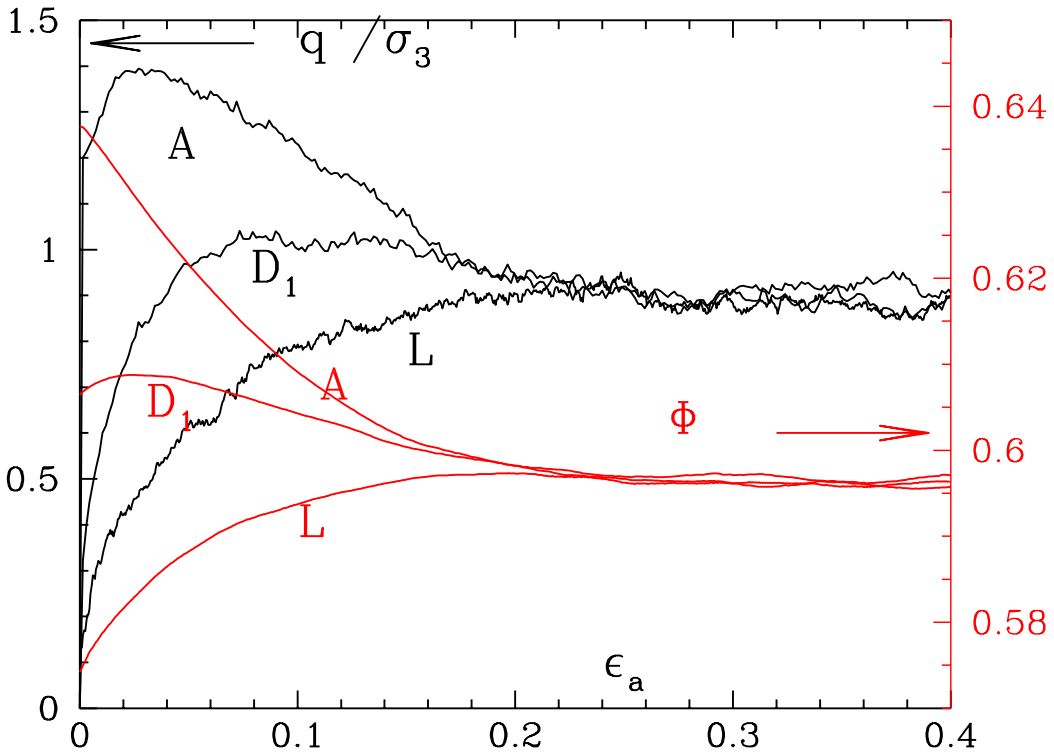

Dense, dilatant (A), intermediate (D1), and loose, contractant (L) samples all approach critical solid fraction Φ and critical deviator plateau at large strains

Approach to critical state: internal variables

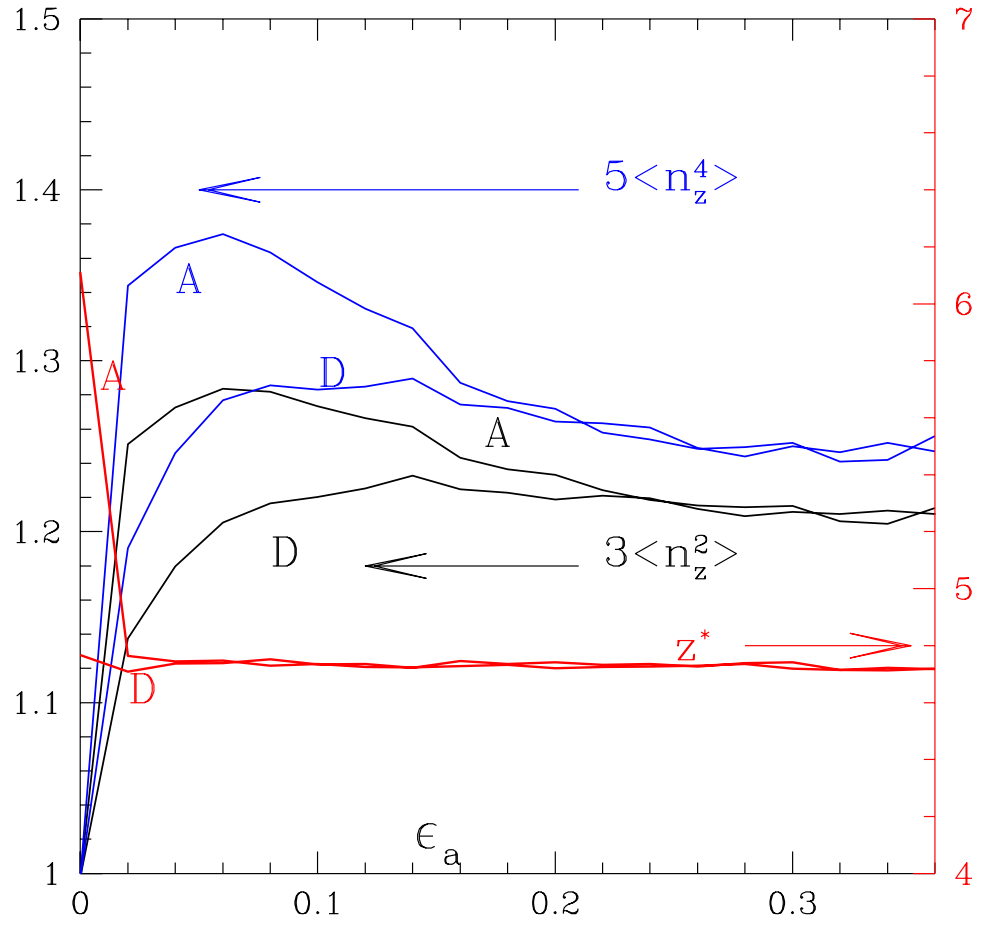

(as also observed by Radjai, Kruyt and Rothenburg...)

Critical state is characterised by specific, “critical” values for coordination number and fabric parameters

Critical state: dependence on friction coefficient

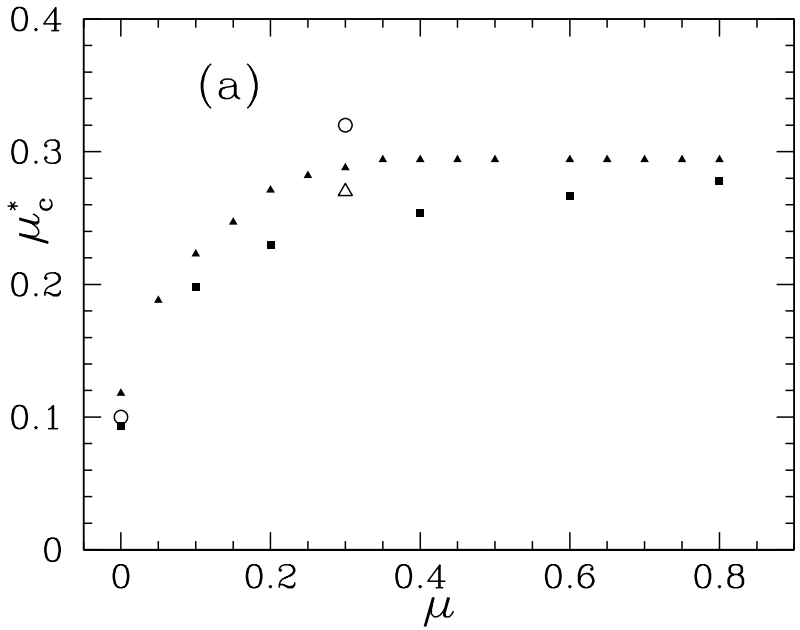

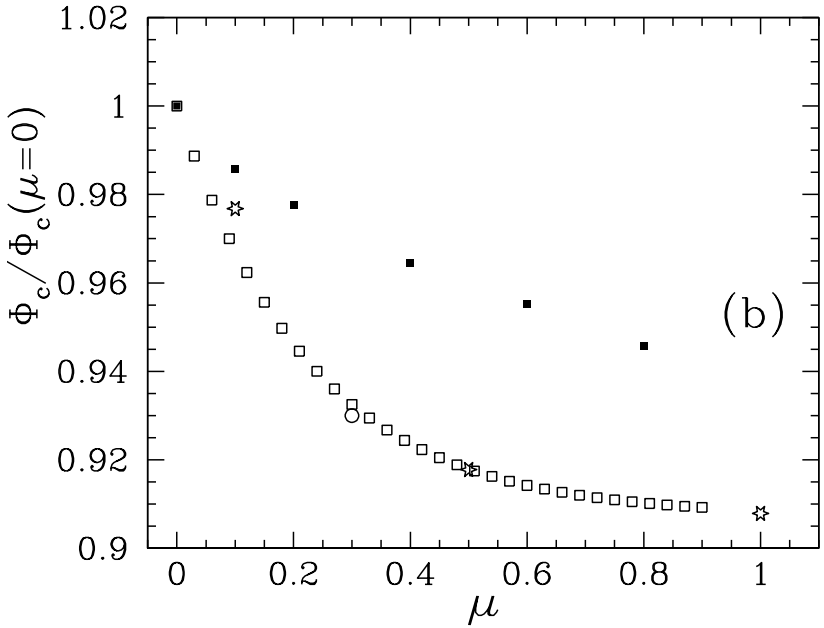

Left: critical internal friction parameter

Right: critical density divided by RCP density

Data from Fazekas *et al.* (Budapest), Estrada *et al.* (Montpellier), UR Navier (our group), Thornton (Birmingham), Campbell (U Southern California). 2D (black dots)/ 3D (open symbols)

Some conclusions

- qualitative features of granular material behaviour, as observed in laboratory, are retrieved
- Microscopic approach and numerical simulations provide insights on influence of initial state (coordination number) and micromechanical features (sliding and rolling friction, particle shape, etc.) on material constitutive behaviour
- Type I/ type II strains to be distinguished.
- Elastic moduli probe microstructure
- Perspectives: we should investigate failure mechanisms and rearrangements (spatial structure, correlations...)